Scaffold Design for Photogrowable Nanonetworks and Pre-Evaluation for Orthogonal Nanoparticle Expansion

---

A Senior Honors Thesis Presented to the

Faculty of the Department of Biology

and Biochemistry

University of Houston

In Partial Fulfillment of the

Requirements for the Degree

Bachelor of Science in

Biochemistry

By

Giovanna Valentina De Vita Sifontes

May 2022

Scaffold Design for Photogrowable Nanonetworks and

Pre-Evaluation for Orthogonal Nanoparticle Expansion

Giovanna Valentina De Vita Sifontes

APPROVED:

Dr. William Widger
Department of Biology and Biochemistry

Dr. Eva M. Harth
Department of Chemistry

Dr. Rita E. Sirrieh
Honors College

Dr. Dan Wells, Dean
College of Natural Sciences and Mathematics

Acknowledgements

The author acknowledges the great contribution of Dr. Eva M. Harth, without whom the opportunity to complete this project would not be possible. Thank you for your faith in me, for your support, for your interest in me, and for agreeing to have me participate in your laboratory group for two semesters while I finished my degree.

Special thanks are attributed to Enkhjargal Tsogtgerel for the enormous support and patience. Thank you for being the awesome mentor that you are, for all your words of wisdom as much as lab-related as life-long lessons. Thank you for being there every step of the way, without you, I would not have made it to the end.

Further thanks go to the entire Harth research group. Thank you for always making me feel welcome, and for answering any type of question that I had. Thank you for cheering me up along the way, and for all the good times.

Thanks to The Office of Undergraduate Research and Major Awards for providing undergraduate students the opportunity to conduct research. Thanks to Dr. Rita Sirrieh and Dr. William Widger for forming part of my Honors Committee.

Finally, I would like to acknowledge the profound encouragement and assistance from my family, friends, and previous professors without whom I would not have made it this far in my career.

Scaffold Design for Photogrowable Nanonetworks and

Pre-Evaluation for Orthogonal Nanoparticle Expansion

An Abstract of Senior Honors Thesis Presented to the

Faculty of the Department of Biology

and Biochemistry

University of Houston

In Partial Fulfillment of the

Requirements for the Degree

Bachelor of Science in

Biochemistry

By

Giovanna Valentina De Vita Sifontes

May 2022

Abstract

A substantial part of polymer chemistry focuses on the formation of block copolymers for functionalization. These polymers possess a wide range of characteristics based on how they are constructed and polymerized. Recently, the focus in this field has shifted to the formation of nanoparticles. Harth's research group has led the way in creating photogrowable nanonetworks (PGNNs). There is an inherent difficulty in conducting orthogonal expansion polymerizations once a PGNN is formed. The challenge of PGNN is to conduct controlled polymerizations that expand either from the scaffold or crosslinker without affecting each other or any end groups. This project covers the formation of various scaffolds for PGNNs with varying properties, and pre-evaluation polymerization reactions involving symmetrical trithiocarbonate crosslinkers to conduct orthogonal polymerizations on nanoparticles involving these scaffolds and crosslinkers. Scaffolds were constructed using reversible-addition fragmentation chain transfer (RAFT) polymerization, or atom transfer radical polymerization (ATRP). The preliminary reactions that tested the crosslinkers were performed with catalyst ZnTPP under green light and with methyl acrylate as the monomer. Several control reactions were performed to examine the orthogonality of the nanonetwork polymerizations. The construction of the scaffolds provided three different designs for expansion methods and different attachment methods for the crosslinkers. Evaluation tests performed on the crosslinkers demonstrated that orthogonal polymerization can be achieved on a PGNN. This project contributed to the formation of three different design scaffolds for future PGNNs and controlled reactions that demonstrate orthogonal expansion of the individual components of photogrowable networks.

Table of Contents

List of Tables

List of Figures

Appendix A: Abbreviations and Acronyms

MMA: methyl methacrylate

FMA: furfuryl methacrylate

ZnTPP: zinc tetraphenylporphyrin

CDTP-OH: 4-cyano-4-[(dodecylsulfanylthiocarbonyl) sulfanyl] pentanol

DMSO: dimethylsulfoxide

d-DMSO: deuterated-dimethylsulfoxide

DCM: dichloromethane

NMR: nuclear magnetic resonance

GPC: gel permeation chromatography

MW: molecular weight / weight average molecular weight

M_n: number average molecular weight

PDI: polydispersity index (Đ)

RAFT: reversible addition fragmentation chain transfer

ATRP: atom transfer radical polymerization

MBPA: methyl α-bromophenylacetate

Me_6Tren: tris[2-(dimethylamino)ethyl]amine

$CuBr_2$: copper (II) bromide

HEMA: (hydroxyethyl) methacrylate

THF: tetrahydrofuran

ROP: ring opening polymerization

MA: methyl acrylate

CPD: 2-cyano-2-propyl benzodithioate

AIBN: 2,2-Azobis (2-methylpropionitrile)

TTC: trithiocarbonate

DTT: 1,4-Dithiothreitol

DMF: dimethylformamide

PTH: 10-phenylphenothiazine

PheoA: pheophorbide A

GENERAL INTRODUCTION

This project focuses on the formation and chain extension of scaffolds and crosslinkers composed of block copolymers by using polymerizations methods such as Atom Transfer Radical Polymerization (ATRP) and Reversible-Addition Fragmentation Chain Transfer (RAFT) Polymerization for the purpose of constructing nanoparticles that can be expanded orthogonally.

I. COPOLYMERS

Copolymers are polymers that are formed by two or more repeating monomers. Block copolymers are a particular type of copolymer; they are different from other copolymers due to a characteristic sequential distribution. Young & Lovell describe block copolymers as linear copolymers with monomers as the repeating units that exist only in long sequences, or blocks, for the same type of monomer species[1]. The most common structures for block copolymers are long sequences of AB, or ABA polymers[1]. Block copolymers possess a variety of properties that depend on the "copolymer sequence distribution, the chemical nature of the blocks, the average molecular weight and the molecular weight distribution of the blocks and the copolymer"[2]. Block copolymers are found ordered or disordered depending on temperature. Incompatibility of structures within the block copolymer gives rise to an "orders microdomain"[3]. There is a wide variety of uses for block copolymers; they range from being utilized on electronics to cosmetics to medicine. However, the most common and continued use for block copolymers has been as thermoplastic elastomers[4]. Given the range of characteristics and applications that can be attributed to block copolymers, the mechanism used for their construction matters to obtain certain qualities. Any preferred method of polymerization depends on the characteristic desired for the block copolymer and for what it is expected to be used for. There has been extensive research on the formation of block copolymers

by as many types of polymerizations as they exist, even by combining different approaches. Most polymerizations of block copolymers follow a "controlled sequential monomer addition"[2].

II. REVERSIBLE-DEACTIVATION RADICAL POLYMERIZATION

The general polymerization method used in this project is Reversible-Deactivation "living" Radical Polymerization, RDRP, from which ATRP and RAFT emanate from. RDRP shares a similar process with free radical polymerization. There are three steps for free radical polymerizations: initiation, propagation, and termination. On the initiation step, an initiator and monomer molecule are present for which the initiator creates a radical species from itself by either homolytic scission or single-electron transfer from an ion or molecule that creates only one free radical species. Homolytic scission, or homolysis, involves the break of a single bond from which each electron is associated with each of the atoms at the ends of the single bond, creating two free radical species. Usually, the presence of heat on a peroxide or azo linkage generates effective initiators[1]. After the formation of the initiator, it attacks a single bond of the monomer to form a radical species that will propagate on the second step. Propagation is the growth of the polymer chain through the monomer with the free radical. It is comprised of the sequential addition of monomers to the chain, which is denoted as a propagating chain. In free radical polymerization, propagation is followed by termination, in which the active species is irreversibly diminished by preventing further propagation, thus, the chain is dead and it can no longer propagate. Termination occurs by the coupling of two free radical species. The death of a chain can occur by multiple scenarios. It is worth noting that there can be chain transfers during the polymerization process[1].

Reversible-deactivation "living" radical polymerization (RDRP), also called controlled radical polymerization (CRP), differs from free radical polymerization by the "omission" of a termination step. The termination step is reversible, and the polymer can "live" again because the

reagents used for these polymerizations can activate and deactivate chains[5]. Therefore, a living chain would also be a propagating chain while a deactivated chain would be in the dormant state but not dead. This permits for RDRP to be especially useful in the formation of vinyl polymers since it allows regulation of the molecular weight, dispersity, end-group fidelity, and design of said polymers[6].

III. NANOPARTICLES

Using RDRP methods such as RAFT and ATRP allows us to construct polymers that can act as scaffolds that can be connected by crosslinkers, forming a nanoparticle or nanonetwork. A nanoparticle is comprised of a scaffold, which for this project, are polymers constructed by RAFT or ATRP, while the crosslinkers used are symmetrical trithiocarbonates (TTCs) that can also polymerize. These crosslinkers can be activated if they possess a RAFT moiety from which monomers can be added, and the scaffold chains can also be extended because of their livingness. The flexibility of RDRP methods lead us to investigate the orthogonality of nanoparticle expansion, that is to say, that an expansion from the scaffold would not affect the crosslinker and vice versa.

Dr. Harth's group has previously demonstrated that nanonetwork crosslinked with symmetrical trithiocarbonate (TTC) agents can expand in size via light-mediated RAFT polymerization[7]. Potentially, a nanonetwork can be expanded either from the scaffold or the crosslinker. This is possible by applying different polymerization techniques and sequential approaches. Depending on the monomer polymerized, the photogrowable nanonetwork (PGNN) can inherit properties such as hydrophobicity, hydrophilicity, and thermosresponsivity, and drastic change in refractive index can be observed[8].

In this work we aim to study the formation of scaffolds and TTC polymerizations for the purpose of refining the expansion from both the crosslinker and the scaffold chain of the nanonetwork utilizing orthogonal conditions. In order to allow for an expansion from both the crosslinker and the scaffold, the scaffold end group has to stay intact during the synthesis of nanonetwork and the conditions to chain extend from both sites should be orthogonal. We envisioned that this could be achieved through orthogonal systems with RAFT[9,10] polymerization, ATRP[11,12], or ROP (Ring opening Polymerization)[13] facilitating scaffolds and TTC crosslinkers.

However, Dr. Harth's group's first generation nanonetwork does not meet the requirement with their RAFT-RAFT nanoparticle as the scaffold end group was intentionally removed to ensure the growth only from the crosslinker. Thus, a chain extension from the scaffold could not happen. Additionally, the post-polymerization modification on the scaffold to facilitate the crosslinking would also degrade the end group[7]. For those reasons, a new crosslinking method is necessary to keep the scaffold end group intact. The new crosslinking method should have conditions, in which no nucleophilic or radical chemistry is involved. Thus, we have three different crosslinking methods in mind that meet those requirements. For a RAFT-RAFT polymer, one method is crosslinking using an isocyanate-alcohol reaction, and the other one is an esterification through acid chloride, while for an ROP-RAFT polymer Diels-Alder (DA) chemistry will be used for crosslinking. Nanoparticle systems different than RAFT-RAFT should be explored because using photocatalysts, like zinc tetraphenylporphyrin (ZnTPP) and pheophorbide A (PheoA), can potentially prohibit a controlled expansion from the scaffold if done after an expansion from the crosslinker due to a single unit monomer insertion into the scaffold end group[9]. Nevertheless, to move forward to apply these crosslinking methods, we first developed different scaffold polymers with monomers with specific chemistries for crosslinking.

MATERIALS

1,4-Dithiothreitol (DTT), 2,2-azobis (2-methylpropionitrile) (AIBN), 2-cyano-2-propyl benzodithioate (CPD), $CuBr_2$, methyl α-bromophenylacetate (MBPA), dimethylsulfoxide (DMSO), triethylamine (TEA), 4-cyano-4-[(dodecylsulfanylthiocarbonyl) sulfanyl] pentanol (CDTP-OH), zinc tetraphenylporphyrin (ZnTPP), as well as all reagents and solvents, were purchased from Sigma Aldrich and used as received unless otherwise stated. An exception was furfuryl methacrylate (FMA) which was obtained from Tokyo Chemical Industry, pheophorbide A (PheoA) was purchased from Cayman Chemical, and Cu(0) was obtained from Alfa Aesar Puratronic (99%, 0.44g/m, gauge 0.25 mm). Acrylate monomers methyl acrylate (MA, 99%), methyl methacrylate (MMA, 99%), 2-hydroxyethyl methacrylate (HEMA, 99%), furfuryl methacrylate (FMA, 95%) were purified immediately before use by passing through a short column of inhibitor removers purchased from Sigma Aldrich. Trithiocarbonates (TTC) 1 & 2, tris[2-(dimethylamino)ethyl]amine (Me_6Tren), and 10-phenylphenothiazine (PTH) were obtained from stock solutions made available by the laboratory.

Some photogrowth polymerizations were performed in a circular glass dish lined with a 400 nm LED strip (390 nm - 405 nm, 24W/5m, from Sunnet RGB purchased from Amazon) and cooled by compressed air. Other photogrowth polymerizations were performed in a circular glass dish lined with a 530 nm LED strip (3600 lumens, 40W, from Sunnet RGB purchased from Amazon) and cooled by compressed air (shown below, A). Other photogrowth polymerizations were performed in front of a light sheet of 680 nm red light custom made with 6 LED's (8 mW) purchased from ThorLab (shown below, B).

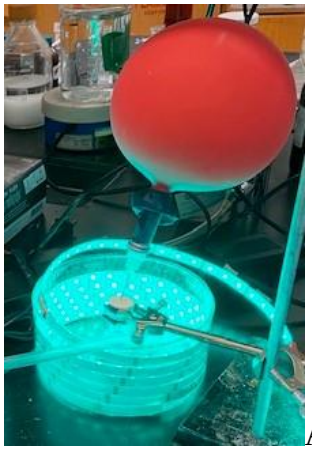
A
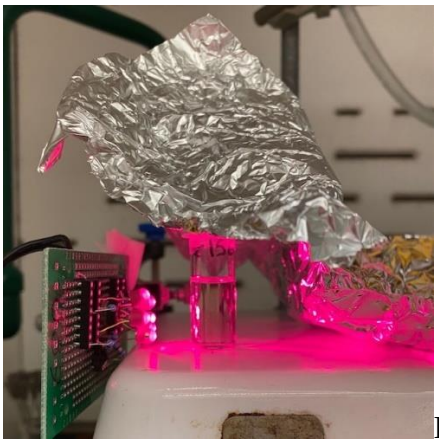
B

Figure M1: Example of a photogrowth polymerization set up. *Notes*: A: example of utilizing a LED light lines glass dish for polymerization. B: example of a red light sheet used for polymerization.

CHARACTERIZATION

All ^{1}H spectra were obtained using a JEOL ECA 400 (400 MHz) spectrometer. Chemical shifts were measured relative to residual solvent peaks as an internal standard set to δ 7.26 ($CDCl_3$), and δ 2.54 (DMSO) for ^{1}H. Gel permeation chromatography (GPC) was performed using a Tosoh high-performance GPC system HLC-8320 equipped with an auto-injector, a dual differential refractive index detector, and TSKgel G series columns connected in series (7.8×300 mm TSKgel G5000Hxl, TSKgel G4000Hxl, TSKgel G3000Hxl). GPC analysis was carried out in HPLC grade tetrahydrofuran (THF) with a flow rate of 1.0 mL/min at 40 °C or N,N-dimethylformamide (DMF) with a flow rate of 10.0 mM LiBr at 40 °C. Molecular weights (M_n and Mw) and molecular weight distributions were calculated from polymethyl methacrylate (PMMA) standards with molecular weights of 800 to 2.2×10^{6} g mol-1 provided by Polymer Standard Service (PSS).

CHAPTER 1: RAFT Scaffold Synthesis and End Group Removal

1.1 Introduction

Reversible-Addition Fragmentation Chain Transfer (RAFT) polymerization is a versatile process by which block copolymers can be constructed; it emanated from RDRP. RAFT polymerization maintains an equilibrium between an active species and a dormant species, but the propagating chain does not create radicals, however, it requires a constant presence of radical monomers that can be achieved by the presence of an initiator like AIBN, for example[14]. Since there is a correlation between the number of dead chains and the number of radical initiators, the number of dead chains can be controlled by the number of radical initiators introduced[15]. RAFT reagents are characterized as thiocarbonylthio groups (ZC(=S)SR) that are responsible for the chain's livingness and controlled polymerization[5].

RAFT polymerization might be preferred over other methods since a varied series of functional monomers and reaction environments can be used[14]. The molecular weight of polymers formed with RAFT can be predicted; these polymers also portray low dispersity (Đ), high end-group fidelity, and capacity for continued chain growth which makes RAFT polymerization an attractive method when a desired block copolymer with certain characteristics is needed[15]. RAFT is also compatible with most reaction conditions, such as organic, aqueous, or protic media, as well as bulk, emulsion, semi-emulsion, or suspension polymerization[5].

The utilization of light to excite and form a radical has been attractive to researchers since it is cheap and permits easy-to-control reactions. Visible light facilitates the formation of radicals that are used to add monomers sequentially[16]. Using light has the advantage of not needing high temperatures for a reaction and minimizes the formation of homopolymers[17]. In effect, using light for polymerization provides fewer side reactions or depolymerization[6]. Using visible light as a

stimulus, is not only cheap, but also easily accessible and does no harm to the environment. Additionally, light offers temporal and spatial control. The perceived drawback of using light as an external stimulus for polymerization, such as scalability concerns and limited depth penetration, have been addressed by the development of flow photochemistry[6].

Polymerization by light and RAFT were combined into PET-RAFT (Photoinduced Electron/Energy Transfer – Reversible-Addition Fragmentation Chain Transfer) polymerization. This type of RDRP merges RAFT, photoredox catalysts, and light as an external stimulus for well-defined polymers that follow environmentally friendly, green chemistry because it draws from the advantages of using light as an external stimulus, the wide availability of catalysts, and the advantages of using RAFT as a polymerization method. A photochemical reaction has the unique ability to switch between an 'on' and an 'off' state; the formation of copolymers is moderated by the continued reuse and recycling of the photocatalysts[18]. A photoiniferter is an involved process which depends on the intensity and wavelength of the visible light as well as the RAFT reagent used since the C-S bond of a trithiocarbonate (TTC), for example, requires low dissociation energy. The photoactivation triggers the electron transfer of the RAFT reagent to start the polymerization, which still allows for a controlled polymerization[19]. This can happen in the presence of air without affecting the reaction[18]. Even though there is not a consensus in the literature on whether the reaction involved in PET-RAFT is an electron or an energy transfer, since there is evidence for both, the literature does agree that PET-RAFT is a unique system that provides for spatial and temporal control while resulting in polymers that are well-defined with narrow dispersities at a relative cheap price[20]. Photoredox catalysts will be further explored in Chapter 2.

PET-RAFT polymerizations do not affect the functionality of the end group[5], however, the end group functionality might interfere with future reactions on the newly synthesized polymer,

for this, end group removal procedures have been devised. This project focused on the removal of the end group using aminolysis. Aminolysis involves the reaction of either ammonia, primary amines, or secondary amines with esters, or thioesters, in a nucleophilic addition-elimination mechanism[21]. Following this mechanism, a thio-ene click reaction occurs for the removal of the end group. Click reactions, such as a thio-ene reaction, have numerous advantages including batch synthesis, simple purification, and little to no byproducts, which is why they are considered highly efficient reactions used in chemical designs and modifications[22]. When the thio-ene reaction is applied to functional end groups of trithiocarbonates (TTC), there are fewer side-reactions, which means that the formation of disulfide interchain coupling or thiolactone formation are reduced[23]. Thus, the end group removal procedure used on this project involved the combination of aminolysis and thio-ene chemistry to produce a thio-terminated polymer.

1.2 Discussion

1.2.1 ROP RAFT Scaffold and End Group Removal

In this project, the scaffold for an Ring Opening Polymerization (ROP) will be constructed in order to use the Diels-Alder (DA) crosslinking chemistry to synthesize a photogrowable nanonetwork (PGNN) capable of expanding through ROP and RAFT polymerization techniques (See Figure 1.1). As the two polymerizations have different mechanisms, this ROP-RAFT system allows us to expand the PGNN from different sites sequentially or in one-pot[13]. The furan bearing scaffold is synthesized from a hydroxy-bearing RAFT agent and the RAFT moiety is subsequently removed. The scaffold is then crosslinked through Diels-Alder reaction by a maleimide bearing TTC crosslinker. The ROP-DA-PGNNs will be expanded from the scaffold using DPP (Diphenyl phosphate) and from the crosslinker using 10-phenylphenothiazine (PTH).

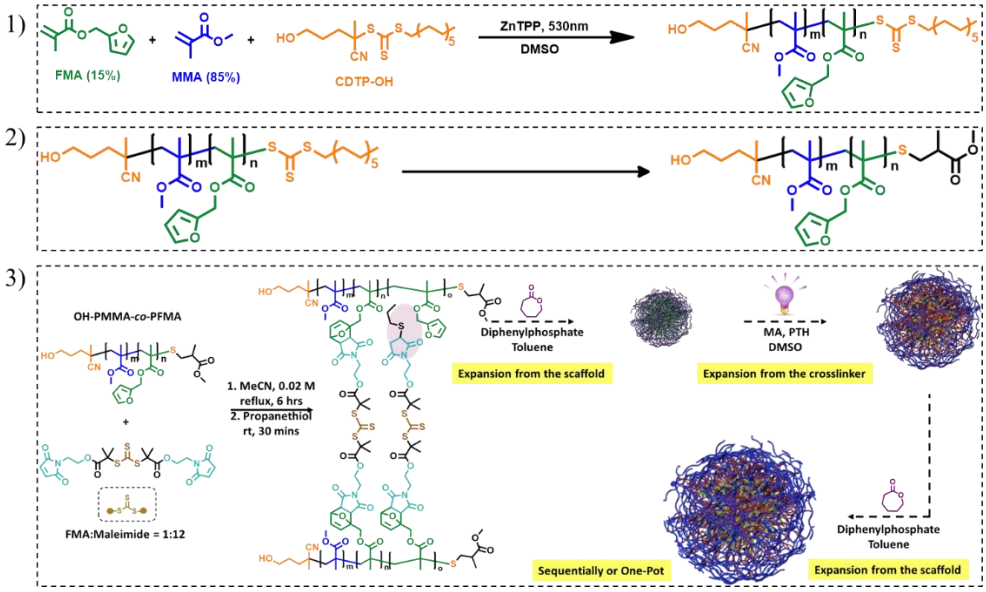

Figure 1.1: Scheme of the overall purpose of ROP PMMA-co-PFMA scaffold with sequence of reactions for the formation and expansion of PGNN. 1) Synthesis of RAFT-PMMA-co-PFMA. 2) End group removal of RAFT-PMMA-co-PFMA. 3) Synthesis and expansion of Ring Opening Polymerization (ROP) Diels-Alder (DA) photogrowable nanonetwork (PGNN).

To obtain the scaffold for this project, we first set out to optimize the RAFT polymerization. We conducted a kinetics study to determine the length for which the reaction should run to obtain a desired molecular weight of 7000 g/mol with a 15% FMA and 85% MMA composition with a homogeneous incorporation of both monomers. The RAFT reagent used for this reaction was CDTP-OH, which was dissolved in DMSO along with MMA and FMA, and ZnTPP as the catalyst. The selectivity of ZnTPP allowed for the reaction to run under light with a wavelength of 530 nm. The kinetics of the reaction was analyzed with ^{1}H NMR every hour for 8 hours, which demonstrated a linear relationship of the incorporation of MMA and FMA into the polymer (see Figure 1.2). The GPC traces at 5, 6, and 8 hours portrayed no termination and no coupling (see Figure 1.3). It was determined that the reaction for the RAFT-PMMA-co-PFMA ROP scaffold should run for 6 hours.

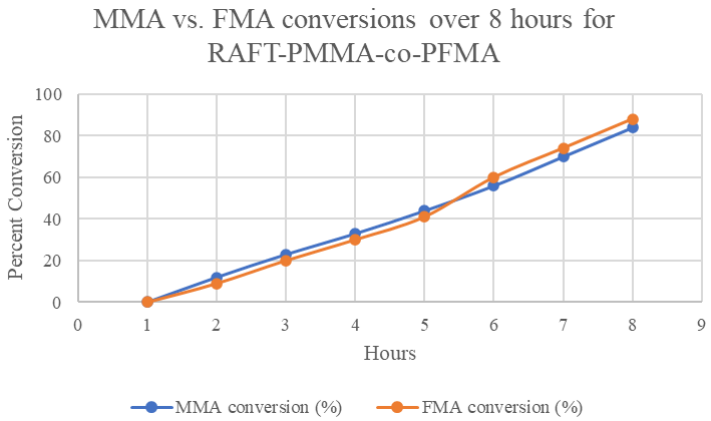

Figure 1.2: MMA and FMA conversion (blue curve and orange curve, respectively) of RAFT-PMMA-co-PFMA ROP scaffold every hour for 8 hours.

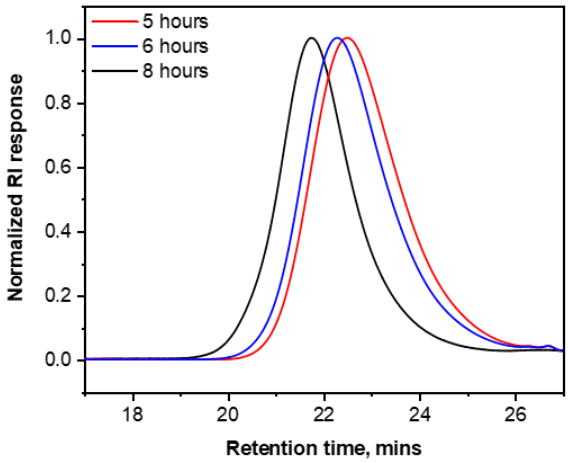

Figure 1.3: $GPC_{(THF)}$ traces of RAFT-PMMA-co-PFMA ROP scaffold at 5 (red), 6 (blue), and 8 (black) hours. Progression through the hours demonstrated an increase in molecular weight by the incorporation of monomer into the chain. Smooth traces portray a homogenous polymer.

Then, we set out to optimize the reaction environment by testing the concentration of monomers in solution. Procedure 1 tested the volume of the solvent, in this case, DMSO, to be equal to the volume of the monomers, while Procedure 2 tested a reaction environment for a 2 M solution of monomer. The GPC trace for Procedure 1 showed a lower dispersity (Đ=1.12) and higher molecular weight ($M_{n,\,GPC}$=7800 g/mol) than Procedure 2 (Đ=1.16, $M_{n,\,GPC}$=7400 g/mol, respectively) (see Figure 1.4). Thus, we decided to continue the reaction environment in which the volume of the solvent was the same as the volume of the monomers. For the subsequent synthesis

of the RAFT-PMMA-co-PFMA scaffold, the reaction was run for 6 hours, with the volume of DMSO equaling the volume of the monomers, and the quantities of the reagents were increased 7.5 times for a yield of 1 g.

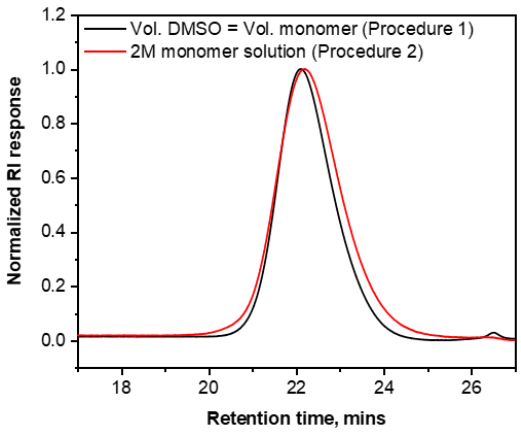

Figure 1.4: $GPC_{(THF)}$ traces of RAFT-PMMA-co-PFMA ROP scaffold when using a volume of DMSO equal to the volume of the monomers (black), and when using a 2 M monomer solution (red).

Next, we focused on optimizing the end group removal of the RAFT-PMMA-co-PFMA scaffold by removing the dithiobenzoate RAFT end group through aminolysis so that the resulting thiol was capped with methyl methacrylate unit to ensure that RAFT polymerization could only occur from the TTC of the crosslinker once the nanonetwork was formed. For Procedure 1, we used a ratio of 1/10/30/30 of RAFT-PMMA-co-PFMA/butylamine/MMA/TEA. The reaction was left running overnight for aminolysis with butylamine and simultaneous thiol-ene reaction with MMA. We used TEA to change any thiols to thiolates for a Michael addition to merge MMA to substitute the RAFT end group. The next day, more butylamine was added to repeat the steps previously mentioned to ascertain that most of the polymers had their end group removed, and the reaction was left overnight. GPC traces of the polymer demonstrated high dispersity (Đ=1.21). Therefore, we decided to try another method for the removal of the end group to examine if the polymer obtained had a lower dispersity with the next method.

The following end group removal procedure (Procedure 2) consisted of three main steps. The first step was to let the reaction running overnight with the RAFT-PMMA-co-PFMA polymer with piperidine and MMA in THF. The piperidine undergoes aminolysis with the thioester. The thiolate product could couple with other thiolates, whose bond would be reduced with 1,4-dithiothreitol (DTT) on the second step. The thiol that forms would react with TEA on the third step, and after a Michael addition with MMA, the end group would be completely removed and replaced by MMA. After looking at the GPC traces, we decided to perform steps 2 and 3 again to ensure the complete removal of the end group. The removal of the end group was confirmed by ^{1}H NMR and a subsequent polymer chain extension demonstrated the livingness of the chains. ^{1}H NMR verified the absence of end group peak after the two rounds of DTT, TEA, and MMA (see Figure 1.5). Additionally, PMMA-co-PFMA scaffold can be chain extended under 400 nm light with PTH as the catalyst, showcasing the high fidelity of the new polymer. In the end, we obtained a functional scaffold polymer from which a crosslinker could be attached through the furan ring of FMA and we could chain extend without affecting the scaffold to perform an ROP from the scaffold.

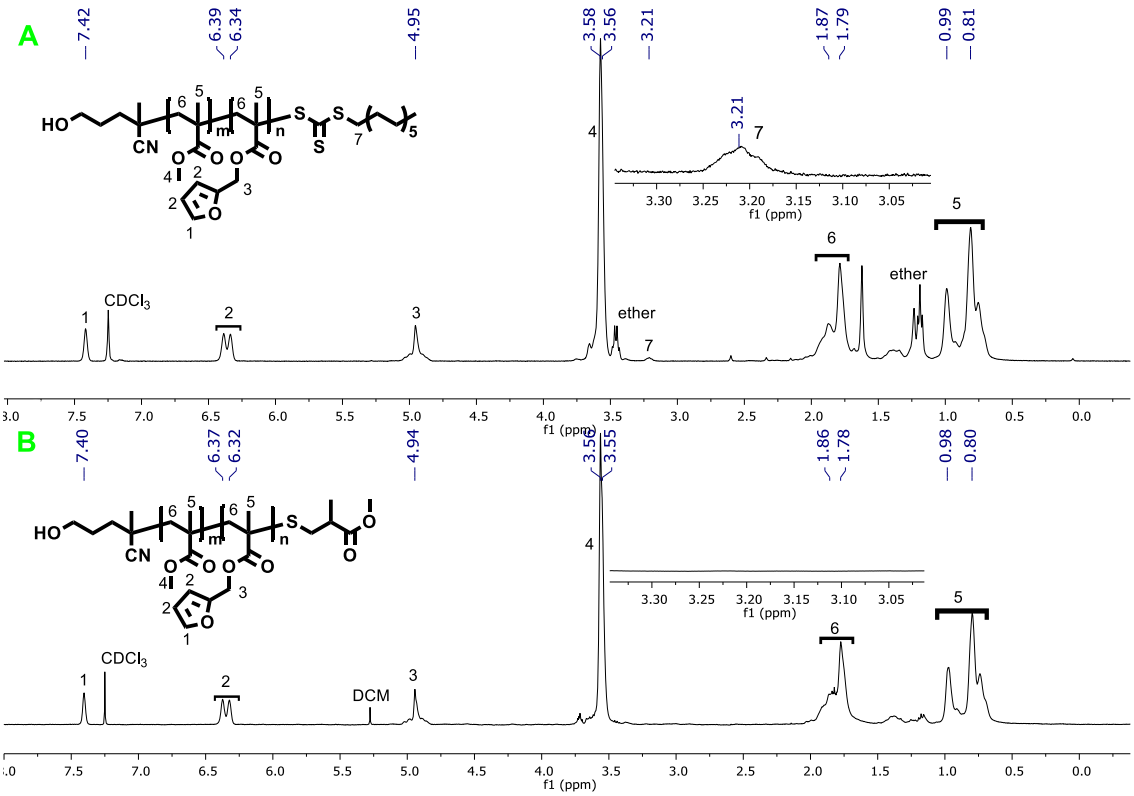

Figure 1.5: ^{1}H NMR comparison before and after end group removal with piperidine and DTT of ROP scaffold. A (top): ^{1}H NMR ($CDCl_3$, 400 MHz) spectrum of the precipitated RAFT scaffold before end group removal (RAFT-PMMA-co-PFMA). B (bottom): ^{1}H NMR ($CDCl_3$, 400 MHz) spectrum of the precipitated RAFT scaffold after end group removal (PMMA-co-PFMA).

Each step to make the PMMA-co-PFMA polymer was optimized to use the scaffold in a nanoparticle that can be expanded through the crosslinker with PET-RAFT and expanded through the scaffold with a ring opening polymerization. The functionality of the furan group on FMA will provide the chemistry necessary through a Diels-Alder reaction to incorporate the TTC crosslinker to form the nanoparticle. The RAFT end group was removed to use the hydroxy, ~OH, for a ring opening polymerization, while the MMA introduced during the end group removal serves as a thiol cap to prevent polymerization through a disulfide bond. This would allow for an orthogonal expansion of the PGNN.

1.2.2 Ester PGNN RAFT Scaffold

In this project, the goal is to explore two different crosslinking chemistry, the isocyanate-alcohol reaction traditionally used in the synthesis of urethanes[24] and esterification through acid chloride. These reactions are attractive due to their reaction rates because higher reaction rates provide better control over nanonetwork size based on concentration and ratio of reagents. Compatibility of the reagents with the RAFT moieties in the scaffold and the crosslinker were tested, and two sets of PGNNs, Isocyanate PGNN and Ester PGNN, will be synthesized after optimizing the conditions. Model experiments utilizing two catalysts PheoA (red light) and ZnTPP (green light) to selectively activate different RAFT moieties in the crosslinker and the scaffold were performed. As it was demonstrated in the literature[9], further proof of the selectivity of the catalysts in our system was obtained. Thus, the PGNNs will be expanded from the crosslinker and from the scaffold utilizing catalysts ZnTPP and PheoA, respectively.

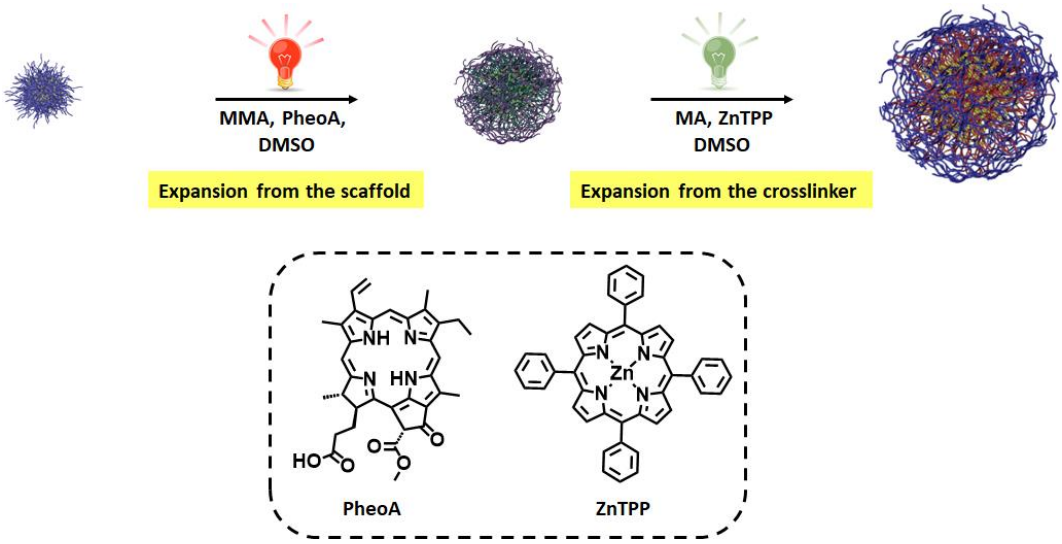

Figure 1.6: Expansions of RAFT-RAFT photogrowable nanonetworks (PGNNs).

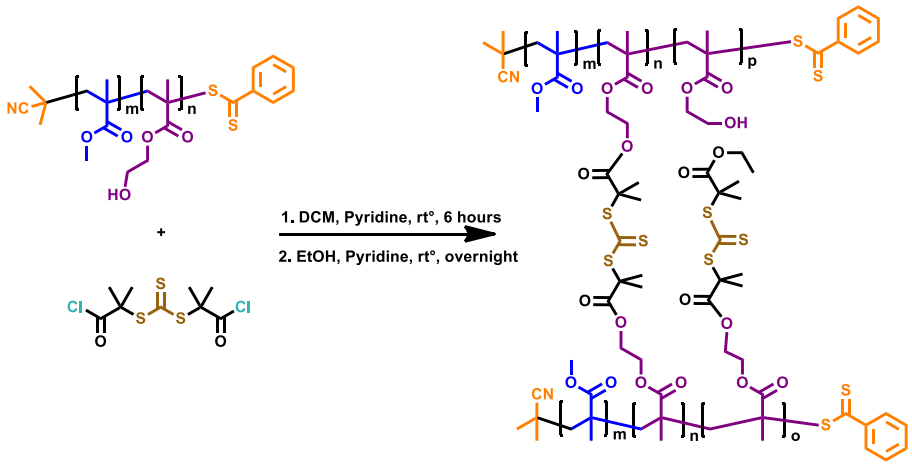

Figure 1.7: Synthesis of ester PGNN.

In order to address the crosslinking concerns on a RAFT-RAFT polymer, we set out to construct a scaffold polymer for an esterification crosslinking chemistry using acid chloride. Our PMMA-co-PHEMA scaffold will provide the alcohol for the esterification with the acid chloride from the crosslinker (acid-chloride TTC1). The PMMA-co-PHEMA RAFT scaffold was constructed for a monomer distribution of 85% MMA and 15% HEMA, with a target molecular weight of 7500 g/mol. For the scaffold, we used MMA and HEMA with CPD as the RAFT reagent and AIBN as the initiator. We used HEMA as one of the monomers for future esterification with acid-chloride TTC1 to form an ester and crosslink two scaffolds. Our RAFT scaffold was 84% MMA and 16% HEMA with a molecular weight of 8600 g/mol and a low dispersity of Đ=1.11.

Next, we conducted a preliminary study of the polymer using the chain extension scaffold condition that would be applied to the nanoparticle. A kinetics study allowed us to observe the polymerization of MMA and chain extension of the scaffold over a period of 24 hours. GPC traces showed consistent low dispersity of the chain extension, and an increase in the molecular weight throughout the 24 hours (see Figure 1.9). Thus, the conditions in which the scaffold will be extended once the nanoparticle is formed were seen to be successful when implemented on the scaffold by itself. The construction of the scaffold and these preliminary tests were necessary to

move forward in the formation of PGNNs and their expansion; the reactions performed will be translated and adapted into the nanonetwork. We can also observe that a photoredox-mediated polymerization provides high fidelity and controlled polymerization, as seen by the consistent low dispersities of this scaffold polymer (Đ ≤ 1.11), as observed in Figure 1.9. The livingness of the chain was conveyed in the GPC traces below for which at 0 hours the polymer was seen with a dispersity of Đ=1.11, and as time progressed, 6, 12, 24 hours, the chain maintained its fidelity with dispersities of Đ= 1.09, 1.10, and 1.10, respectively.

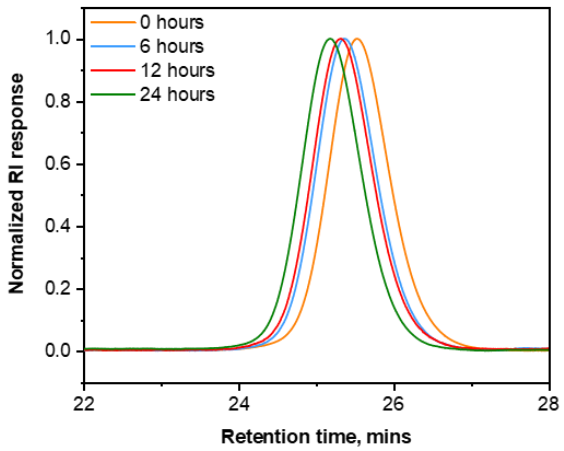

Figure 1.8: $GPC_{(DMF)}$ traces of PMMA-co-PHEMA-b-PMMA scaffold polymer before polymerization (yellow), at 6 (blue), 12 (red), and 24 (green) hours.

1.3 Conclusion

Two scaffolds were synthesized using RAFT polymerization. The first scaffold, PMMA-co-PFMA, was synthesized to be part of a nanoparticle that will be extended from the scaffold by ROP while being crosslinked by a Diels-Alder reaction for a crosslinker that will be expanded using RAFT. A kinetics study was performed in order to examine monomer conversion and progression of the polymerization. From this study, we determined a reaction running time of 6 hours. Then, we set out to optimize the reaction environment by comparing the ratio of the volume of the solvent to the monomers. It was suggested that a reaction environment containing the same

amount of volume of DMSO as volume of the monomers had a lower dispersity (Đ=1.12) than an environment of a 2M monomer solution (Đ=1.16). The quantities of the reagents were upscaled 7.5 times for subsequent syntheses. Next, we optimized the end group removal procedure by aminolysis. We decided to follow a procedure containing piperidine and DTT over a procedure with butylamine and TEA since the resulting polymer did not have an end group present (as observed by ^{1}H NMR) and lower dispersity. The polymer would now be ready to form part of a nanoparticle with the desired chemistry.

The second type of scaffold prepared using RAFT polymerization, PMMA-co-PHEMA, would be used to form an Ester PGNN. The scaffold was synthesized with CPD as the RAFT reagent and AIBN as the initiator. The polymer was subjected to evaluation of the scaffold chain extension conditions of the ester nanoparticle, for which a kinetics study was performed. The kinetics study portrayed consistent low dispersity (Đ≤1.11), and the livingness of the chain.

1.4 Experimental

1.4.1 Synthesis of ROP Scaffold (RAFT-PMMA-co-PFMA)

1.4.1.1 Kinetics and synthesis of RAFT-PMMA-co-PFMA

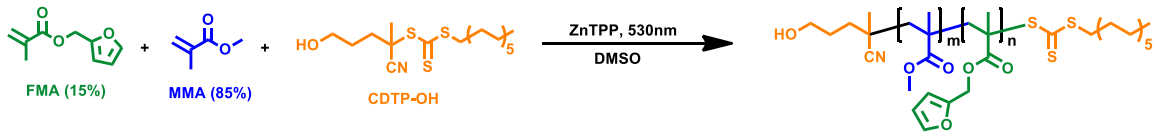

For a target molecular weight of 7000 g/mol with 15% FMA and 85% MMA, CDTP-OH (71.64 mg, 0.184 mmol) was dissolved in a 1 dram vial containing MMA (1 mL, 9.389 mmol), FMA (255 µL, 1.657 mmol), 50 ppm of the monomers of ZnTPP, the same volume of the monomers of DMSO. The reaction vessel was sealed and sparged with nitrogen for 20 minutes. An argon balloon was attached. The reaction was then placed 2 cm from a 530 nm led light source and irradiated for 8 hours. At every hour, an aliquot for ^{1}H NMR characterization was taken. After

the 8 hours passed, the reaction was analyzed by $GPC_{(THF)}$ ($M_{n,\ GPC}$ =8900 g/mol, Đ=1.23, $M_{n,\ NMR}$ = 7400 g/mol).

Hour	MMA conversion (%)	FMA conversion (%)
1	0	0
2	12	9
3	23	20
4	33	30
5	44	41
6	56	60
7	70	74
8	84	88

Table S1.1: MMA and FMA conversion of RAFT-PMMA-co-PFMA ROP scaffold every hour for 8 hours. Monomer conversion determined from ^{1}H NMR

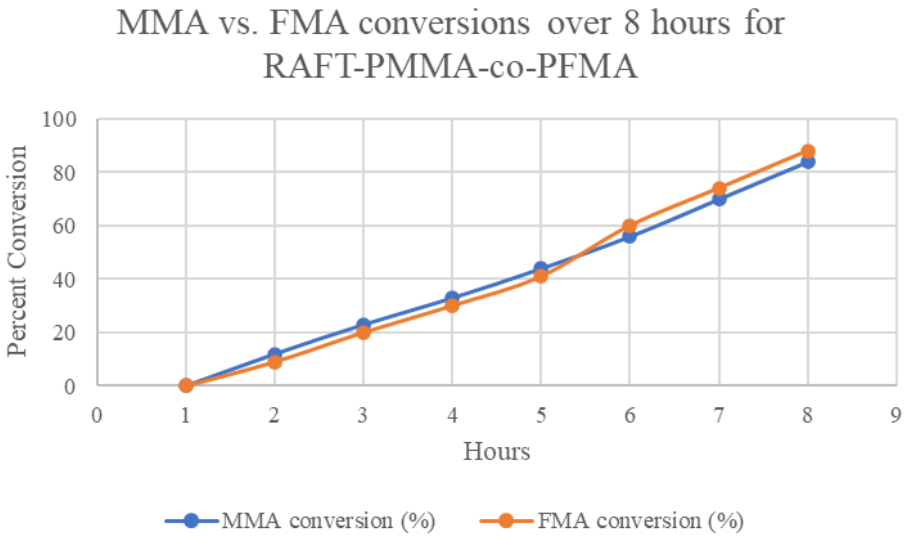

Figure S1.1: MMA and FMA conversion (blue curve and orange curve, respectively) of RAFT-PMMA-co-PFMA ROP scaffold every hour for 8 hours.

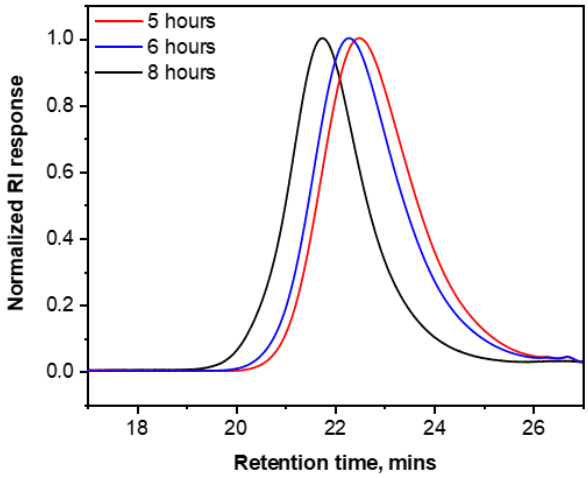

Figure S1.2: $GPC_{(THF)}$ traces of RAFT-PMMA-co-PFMA ROP scaffold at 5 (red), 6 (blue), and 8 (black) hours.

1.4.1.2 Procedure optimization for ROP scaffold (RAFT-PMMA-co-PFMA)

1.4.1.2.1 Procedure 1: Volume of DMSO = Volume of monomers

CDTP-OH (28.66 mg, 0.0735 mmol) was dissolved in a 1 dram vial containing MMA (400 µL, 3.755 mmol), FMA (102 µL, 0.662 mmol), 50ppm of the monomers of ZnTPP, the same volume of the monomers of DMSO. The reaction vessel was sealed and sparged with nitrogen for 20 minutes. The reaction was then placed 2 cm from a 530 nm led light source and irradiated for 6 hours. The polymer was precipitated in methanol and dried under high vacuum to be analyzed by $GPC_{(THF)}$.

1.4.1.2.2 Procedure 2: 2 M monomer solution

CDTP-OH (28.66 mg, 0.0735 mmol) was dissolved in a 1 dram vial containing MMA (400 µL, 3.755 mmol), FMA (102 µL, 0.662 mmol), 50 ppm of the monomers of ZnTPP, the amount of DMSO added to make a 2 M monomer solution. The reaction vessel was sealed and sparged with nitrogen for 20 minutes. The reaction was then placed 2 cm from a 530 nm led light source and irradiated for 6 hours. The polymer was precipitated in diethyl ether and dried under high vacuum to be analyzed by $GPC_{(THF)}$.

	M_n (g/mol)	Đ
Vol. DMSO = Vol. monomers	7800	1.12
2M monomer solution	7400	1.16

Table S1.2: Molecular weight and dispersity obtained from $GPC_{(THF)}$ traces of RAFT-PMMA-co-PFMA ROP scaffold when using a volume of DMSO equal to the volume of the monomers, and when using a 2M monomer solution

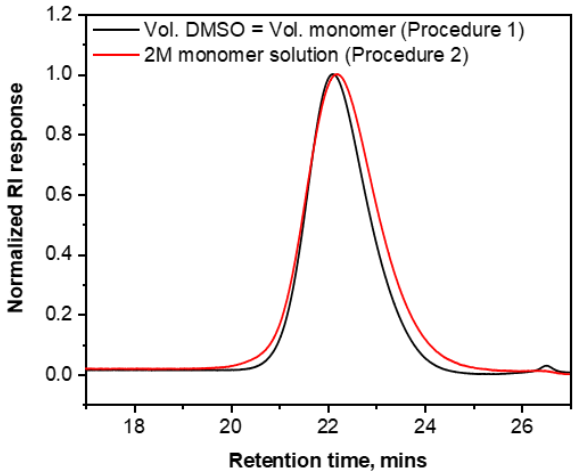

Figure S1.3: $GPC_{(THF)}$ traces of RAFT-PMMA-co-PFMA ROP scaffold when using a volume of DMSO equal to the volume of the monomers (black), and when using a 2M monomer solution (red).

1.4.1.3 Optimization of end group removal procedure (PMMA-co-PFMA)

1.4.1.3.1 Procedure 1: End group removal by using butylamine and triethylamine

RAFT-PMMA-co-PFMA/butylamine/MMA/triethylamine ratio was equal to 1/10/30/30. 500 mg of the RAFT-PMMA-co-PFMA (85%/15%) polymer (0.068 mmol) and 217 µL of MMA (2.04 mmol) in 9mL of THF were dissolved in a 25 mL round bottom flask with a stir bar. While 67 µL of butylamine (0.67 mmol), 284 µL of TEA (2.04 mmol), and 1 mL of THF were combined in a 1 dram. Both vessels were sealed and Freeze-Pump-Thaw (F-P-T) three times. The contents of the 1 dram were added to the round bottom flask while both vessels had an attached argon

balloon. The reaction was left overnight. More butylamine (67 µL) was added the next day and it was left overnight. The reaction was analyzed by $GPC_{(THF)}$ ($M_{n,\,GPC}$ =7800 g/mol, Đ=1.21).

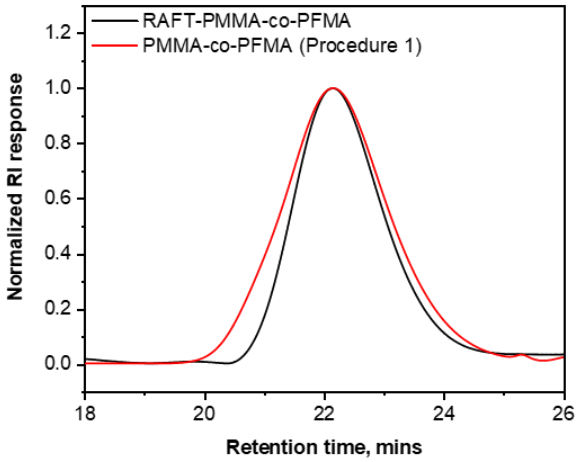

Figure S1.4: $GPC_{(THF)}$ traces of RAFT-PMMA-co-PFMA (black) and PMMA-co-PFMA from procedure 1 of the end group removal (red).

1.4.1.3.2 Procedure 2: End group removal by using piperidine and DTT

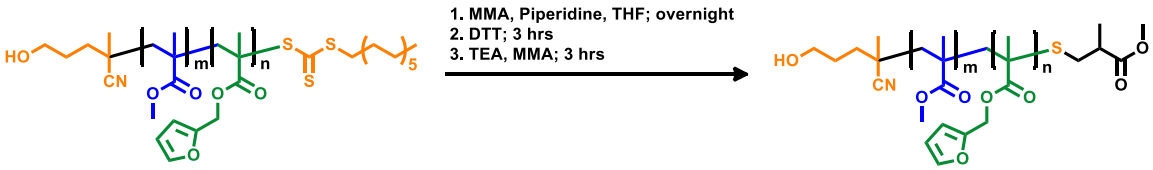

RAFT-PMMA-co-PFMA/MMA/piperidine ratio was equal to 1/23.5/12. 450 mg of the PMMA-co-PFMA (85%/15%) polymer (0.068 mmol) were dissolved in 4.5 mL of THF in a 4 dram with a stir bar. On a 1 dram, 170 µL of MMA (1.596 mmol) and 80 µL of piperidine (0.8099 mmol) were incorporated along with 0.5 mL of THF. Both vessels were sealed and Freeze-Pump-Thaw (F-P-T) three times. The contents of the 1 dram were added to the 4 dram drop by drop. The reaction was left to stir overnight. The next day, the reaction was transferred to a 6 dram for the solvent to be reduced under pressure. After that, it was precipitated in diethyl ether. The remnants of the precipitation were redissolved in THF, and 80 µL of piperidine were added for the reaction to be stirred overnight. An aliquot was taken for $GPC_{(THF)}$ analysis ($M_{n,\,GPC}$ =7500 g/mol, Đ=1.24).

15.6 mg of DDT (~0.1 mmol) were added to the reaction and stirred for 3 hours. After the 3 hours passed, 15 µL of TEA (0.108 mmol) and 170 µL of MMA were added and the reaction was stirred for another 3 hours, after which it was precipitated in diethyl ether for $GPC_{(THF)}$ analysis ($M_{n,\ GPC}$ =9900 g/mol, Đ=1.14). The remnants of the precipitation were redissolved in 5 mL THF to which 15.8 mg of DTT (~0.1 mmol) were added and stirred for 3 hours. After the 3 hours passed, 15 µL of TEA and 170 µL of MMA were added and the reaction was stirred for another 3 hours, after which it was precipitated in cold diethyl ether for $GPC_{(THF)}$ analysis ($M_{n,\ GPC}$ =10800 g/mol, Đ=1.11)

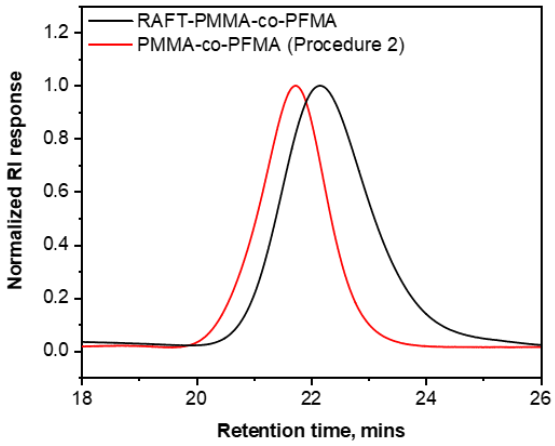

Figure S1.5: $GPC_{(THF)}$ traces of RAFT-PMMA-co-PFMA (black) and PMMA-co-PFMA from procedure 2 of the end group removal (red).

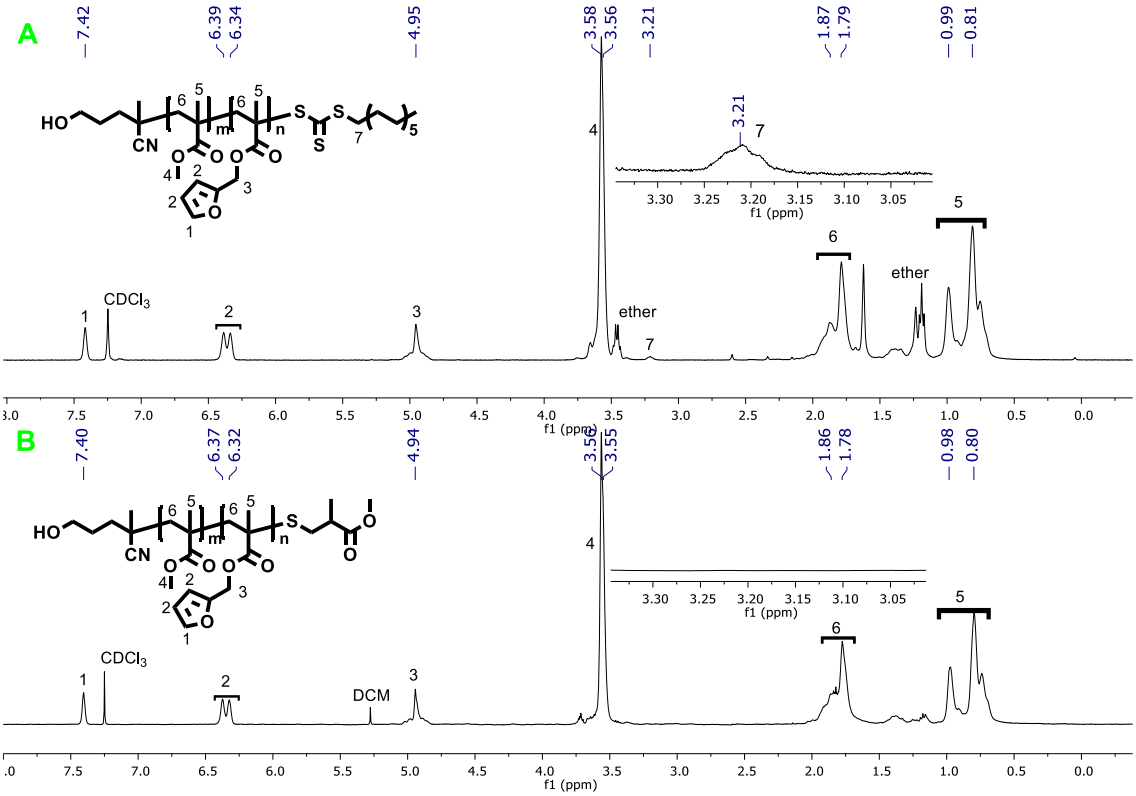

Figure S1.6: A (top): ^{1}H NMR ($CDCl_3$, 400 MHz) spectrum of the precipitated RAFT scaffold before end group removal (RAFT-PMMA-co-PFMA). B (bottom): ^{1}H NMR ($CDCl_3$, 400 MHz) spectrum of the precipitated RAFT scaffold after end group removal (PMMA-co-PFMA).

- Molecular weight, FMA %, and FMA repeat unit calculations of RAFT-PMMA-co-PFMA from ^{1}H NMR.

Peak 7, belonging to the RAFT end group, on the above ^{1}H NMR graphic was integrated to 2 (δ 3.13 – δ 3.26), which gave integration of peak 1, belonging to FMA, (δ 7.48 – δ 7.34) as 10.55 and integration of peak 4, belonging to MMA (δ 3.68 – δ 3.49) as 156.48. Since peak 1 represents only 1 ^{1}H, then the value of integration is divided by 1 (10.55/1 = 10.55). Equally, since peak 4 represents 3 ^{1}H, then the value of integration is divided by 3 (156.48/3 = 52.16). Thus, the calculation continues as follow:

1 CDTP-OH + (10.55*MW FMA) + (52.16*MW MMA)

389.68 + (10.55*166.17) + (52.16*100.12) = 7365 g/mol

% FMA = $\frac{10.55}{10.55+52.16}$ = 17% FMA

FMA Repeat Unit = $\frac{7365\ \text{g/mol}}{10.55}$ = 698 g/mol

1.4.2 Synthesis of Ester PGNN RAFT scaffold (PMMA-co-PHEMA)

1.4.2.1 Synthesis of PMMA-co-PHEMA with CPD

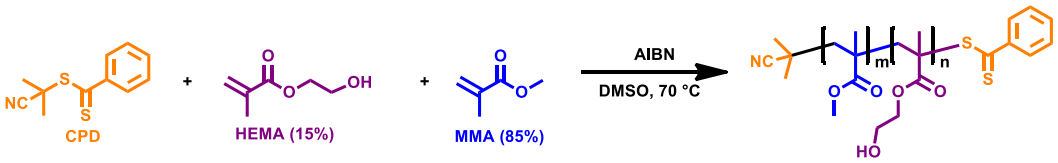

For a target molecular weight of 7500 g/mol with 85% MMA and 15% HEMA, the following procedure was followed. HEMA (603 µL, 1.6568 mmol), MMA (3 mL, 9.3887 mmol), CPD (105.4 mg, 0.1588 mmol), AIBN (11.7 mg, 0.0238 mmol) were dissolved in DMSO (3.603 mL). The reaction vessel was sealed and sparged with nitrogen for 20 minutes. The reaction was then placed on a 70 ºC oil bath for 14 hours. The polymers were precipitated in cold diethyl ether twice, and then analyzed by $GPC_{(DMF)}$ ($M_{n,\ GPC}$ =8600 g/mol, Đ=1.11, $M_{n,\ NMR}$ =7803 g/mol, MMA=84%, HEMA=16%).

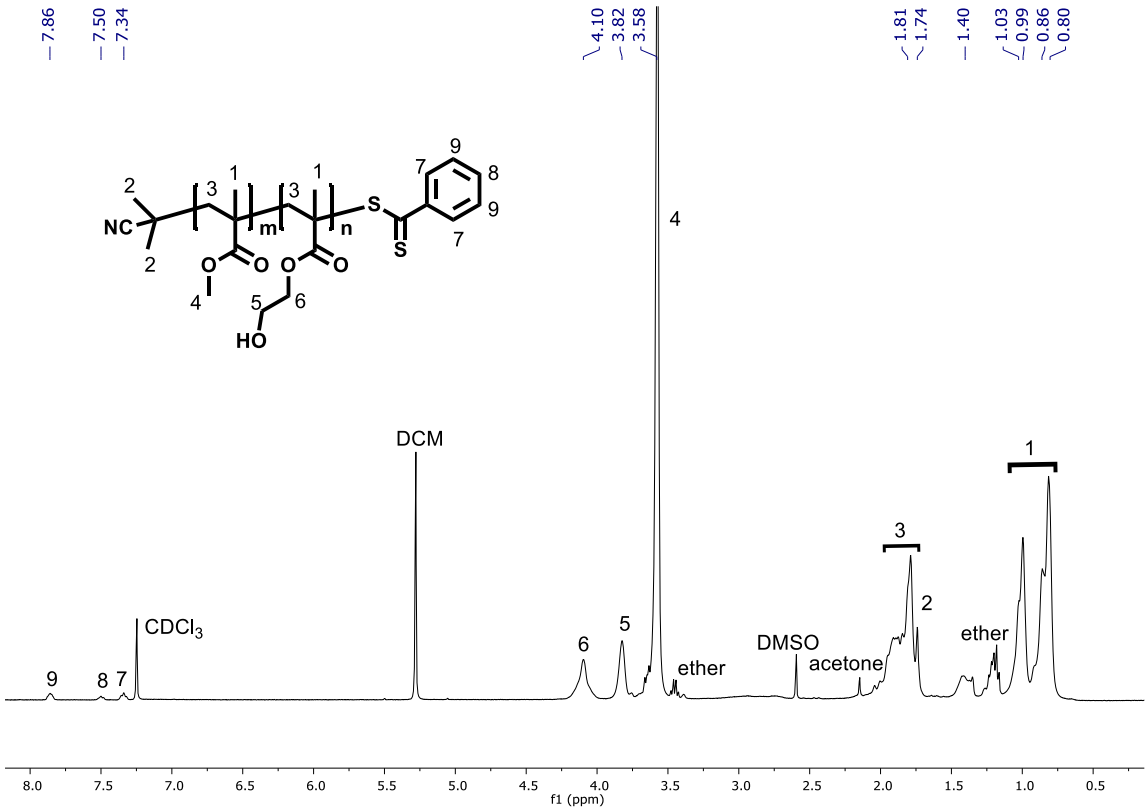

Figure S1.7: ^{1}H NMR ($CDCl_3$, 400 MHz) spectrum of the precipitated RAFT scaffold (PMMA-co-PHEMA).

- Molecular weight, HEMA %, and HEMA repeat unit calculations of PMMA-co-PHEMA RAFT Scaffold from ^{1}H NMR.

Peak 9, belonging to the RAFT end group, on the above ^{1}H NMR graphic was integrated to 2 (δ 7.90 – δ 7.80), which gave integration of peak 6, belonging to HEMA, (δ 4.24 – δ 3.95) as 22.56 and integration of peak 4, belonging to MMA (δ 3.71 – δ 3.49) as 183.18. Since peak 1 represents 2 ^{1}H, then the value of integration is divided by 2 (22.56/2 = 11.28). Equally, since peak 4 represents 3 ^{1}H, then the value of integration is divided by 3 (183.18/3 = 61.06). Thus, the calculation continues as follow:

1 CPD + (11.28*MW HEMA) + (61.06*MW MMA)

221.34 + (11.28*130.14) + (61.06*100.12) = 7803 g/mol

% HEMA = $\frac{11.28}{11.28+61.06}$ = 16% HEMA

HEMA Repeat Unit = $\frac{8473\ g/mol}{12.235}$ = 692 g/mol

1.4.2.2 RAFT scaffold PMMA-co-PHEMA chain extension

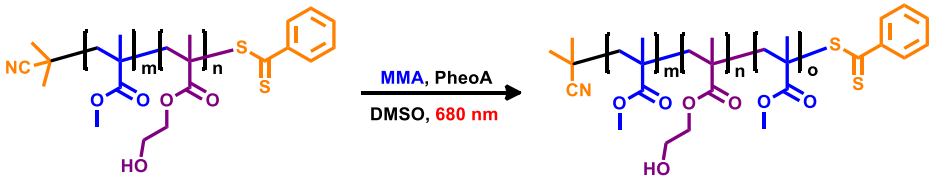

PMMA-co-PHEMA scaffold polymer (20 mg, 0.00256 mmol) was dissolved in 2 M monomer solution in DMSO with MMA (109.2 µL, 1.025) and PheoA (2 ppm to the monomer) in a 1 dram vial. The reaction vessel was sealed and sparged with nitrogen for 20 minutes. The reaction was then placed 1.5 cm from a 680 nm led light source and irradiated for 24 hours. Aliquots were taken at 0, 6, 12, and 24 hours for $GPC_{(DMF)}$ analysis (Đ= 1.11, 1.09, 1.10, 1.10, respectively).

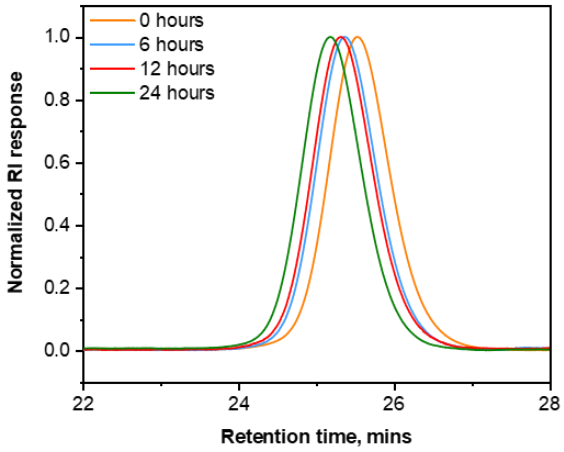

Figure S1.8: $GPC_{(DMF)}$ traces of PMMA-co-PHEMA-b-PMMA scaffold polymer before polymerization (yellow), at 6 (blue), 12 (red), and 24 (green) hours.

CHAPTER 2: Crosslinker Polymerization and Control Experiments for Orthogonal Polymerization

2.1 Introduction

The beginning of crosslinker chemistry started with the formation of single-chain nanoparticles (SCNPs), which involved intramolecular linking. A single polymer chain can link with itself by homofunctional collapse, heterobifunctional collapse, or crosslinker-mediated collapse[25]. Even though this crosslinking happens intramolecularly, it gave rise to the crosslinker chemistries involved in intermolecular crosslinking, as the one used to form photogrowable nanonetworks (PGNNs). There are three main approaches for crosslinking chemistry: irreversible covalent, reversible (dynamic) covalent, and noncovalent. Click chemistry, radical coupling, and Diels-Alder ligation are examples of irreversible covalent crosslinking strategies that help with the stability of the nanonetwork[25].

Crosslinking between two entities can create defects on the nanonetwork and affect its reactivity and dynamic. However, perfecting crosslinker chemistries allows for better control of repairs, reconstructions, and changes on the topology of the nanonetwork[8]. For this project, crosslinkers are composed of symmetrical trithiocarbonates (TTCs) that can participate in photogrowth with photoredox catalysts. These TTC crosslinkers are characterized as macroinitiators that allow expansion of the chain, producing daughter nanoparticles that can convey new properties that differ from their parent nanoparticle[8]. Particular TTCs behave as iniferters when they are photoresponsive because they rely on a light source and do not require an exogenous source of radical initiator[7]. ABA tirblocks and ABABA pentablocks could potentially be produced when TTCs are symmetrical; this expansion is possible because the TTC is already integrated into the nanonetwork via the crosslinker, allowing for unique topology architectures of

linear polymers. This permits control over the manipulation of physical and chemical properties, which can allow changes from the parent nanoparticle to the daughter nanoparticle[8].

PET-RAFT photogrowth from TTC crosslinkers is possible by the presence of photoredox catalysts, such as ZnTPP and PheoA. The photoredox catalyst gets excited by the light source, triggering the electron transfer that activates the RAFT moiety which generates propagating radicals that quickly recombine into dormant chains. The reduction-oxidation chemistry of the catalysts is compatible with the 'on' and 'off' characteristic of PET-RAFT. They also provide stability and spatiotemporal control[19].

Highly effective PET-RAFT photoredox catalysts are metalloporphyrins, like ZnTPP which favor trithiocarbonates over thiocarbonylthio compounds. Interactions between sulfur and zinc are observed in biochemistry for redox-active coordination in the protein motif of zinc fingers, which are involved in DNA recognition during transcription. Using ZnTPP as a photoredox catalyst is advantageous because the polymerization reaction can be carried out in the presence of oxygen, and it can activate PET-RAFT at specific wavelengths, which also permits control of polymerization rate[10]. The selectivity portrayed by ZnTPP is supremely valuable for orthogonal polymerization since it grants polymerization under specific conditions, which could be applied either to the scaffold or the crosslinker. PheoA possesses a similar chemistry to that of ZnTPP[19].

2.2 Discussion

2.2.1 Crosslinker Polymerization

Individual evaluation of the crosslinkers, TTC1 and TTC2, was performed in order to determine and predict their behavior once they were incorporated into the nanoparticle. The polymerization environment was performed according to the same environment projected to be used once TTC1 and TTC2 were incorporated into their respective nanoparticles, Ester PGNN and

Isocyanate PGNN, respectively. These crosslinkers will provide an expansion of the particle through RAFT polymerization, which depending on the type of nanoparticle they form part of, might be a different polymerization condition than the expansion of the scaffold. The following pre-evaluation polymerizations with the crosslinkers will predict polymerization rate and control, dispersity, and monomer conversion.

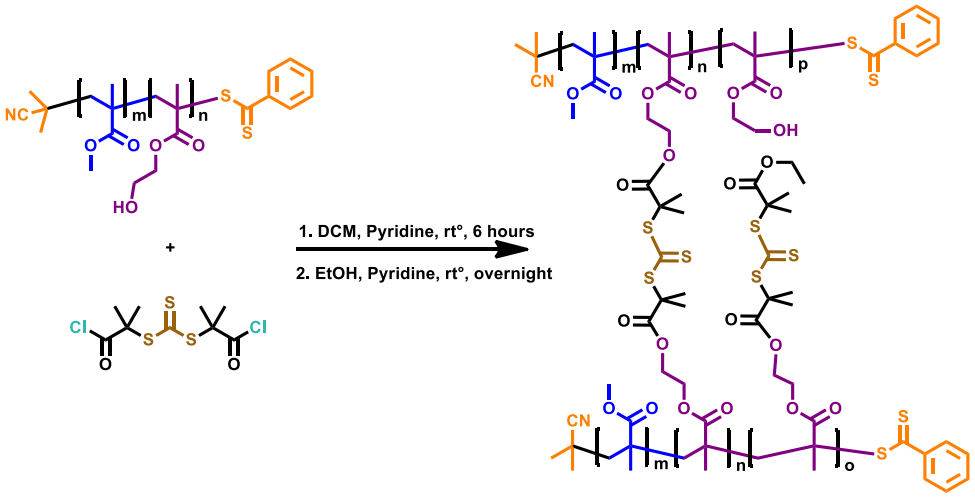

Figure 2.1: Synthesis of ester PGNN.

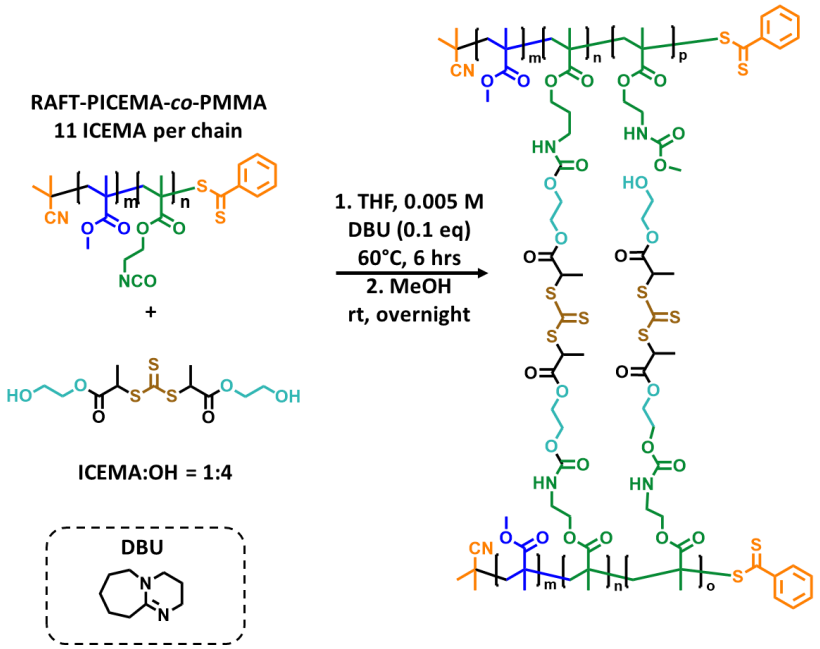

Figure 2.2: Synthesis of isocyanate PGNN.

We conducted preliminary studies of the crosslinkers (TTC1 and TTC2) to observe the continuous incorporation of monomer, and to know the duration of polymerization to extend a chain under the environment of those TTCs. We used a modified version of the crosslinker for the ester PGNN, TTC1, because the acid chloride crosslinker was too unstable. We decided to test both TTCs with MA because of their flexibility to be polymerized in DMSO and provide good control over dispersity. The conditions used to extend the crosslinker, PMA polymerization with ZnTPP as a catalyst under 530 nm light, were applied to TTC1 and TTC2 since they will both be used as crosslinkers for nanonetworks. Both TTCs portrayed homogenous and linear MA conversion, as observed by ^{1}H NMR (see Figure 2.3). TTC1 maintained a low, consistent dispersity throughout the conversion, which was almost the same as TTC2, except that the PDI of TTC2 at 30 minutes was slightly higher than TTC1's (Đ= 1.14, 1.09, respectively). Molecular weight data obtained from GPC showed continuous increase for both crosslinkers over time. GPC traces demonstrated no termination and no coupling as well as a continuous monomer incorporation for both TTCs (see Figure 2.4).

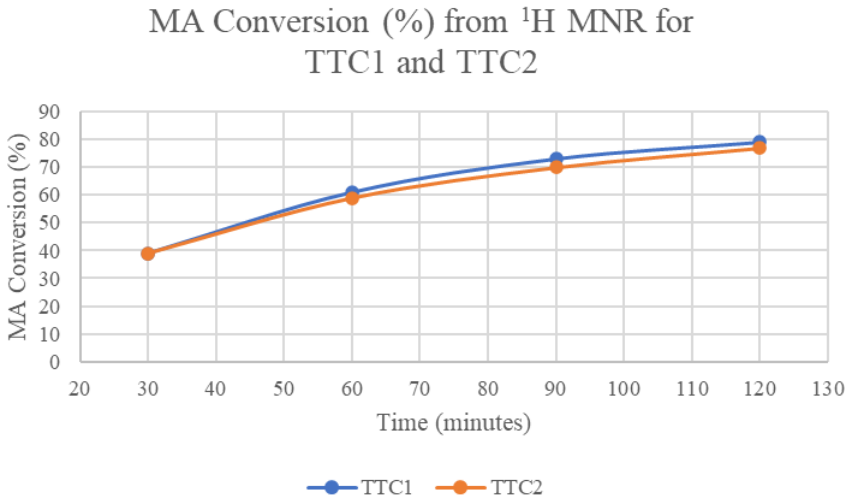

Figure 2.3: MA conversion percentage of TTC1 and TTC2 taken every 30 minutes for 2 hours from ^{1}H NMR.

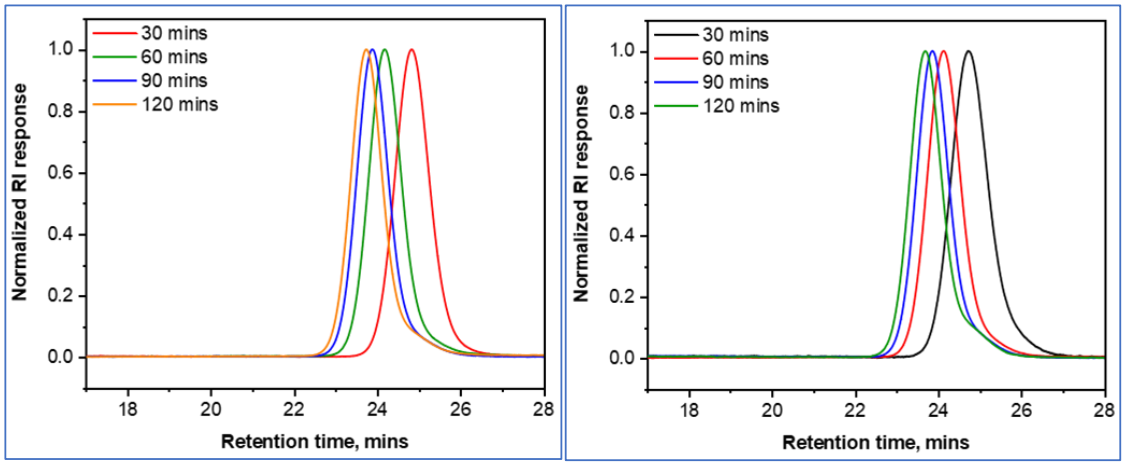

Figure 2.4: Side by side GPC traces of TTC1 and TTC2 kinetics. On the left, $GPC_{(DMF)}$ traces of PMA polymerization with TTC1 and ZnTPP every 30 minutes for 2 hours. On the right, $GPC_{(DMF)}$ traces of PMA polymerization with TTC2 and ZnTPP every 30 minutes for 2 hours.

The chain extension performed after the PMA polymerization with TTC1 conveyed that even if there was an incorporation of a monomer before or the polymer was chain extended before, we can continue to chain extend a polymer with TTC1 after we stopped polymerization and purified the product. This demonstrates high fidelity and livingness of TTC1 since it confirms that every chain remains active.

We investigated the reactivity of both crosslinkers in an isolated environment to examine their behavior before they were incorporated into a nanoparticle. Since there is monomer incorporation (for TTC1 and TTC2) and chain extension (for TTC1) outside of them being in the nanoparticle we suggest that if polymerization/chain extension does not happen in the particle is because of something else, not because the TTCs are not able to polymerize MA, which is why we conducted these preliminary tests. By applying these preliminary studies, we concluded that the conditions from which we anticipate expanding the nanoparticle from the crosslinker, do work independently with the crosslinkers.

2.2.2 Control Experiments for Orthogonal Polymerizations

Several control experiments were performed to observe if the reactivities of catalysts or RAFT reagents could interfere with polymerization independently of each other. Within 24 hours, there was little to no polymerization in the presence of TTC1 and MA, TTC2 and MA, CPD and MMA, and PheoA and MMA (Reference Table S2.3 on the Experimental (2.4) section). There was a relatively high monomer conversion when ZnTPP was analyzed (30% MA conversion), however, the reaction was performed for 24 hours when most of the reactions using ZnTPP are run for 6 hours maximum. Thus, we conclude that in most of the polymerizations in which ZnTPP is present, the polymerization occurs by reaction of the RAFT reagent and catalyst, and not because ZnTPP is the only polymerizing agent.

Each reaction was performed under the same environment as the polymerizations would be run, except that the reaction environment had either the RAFT reagent or the catalyst. Reactions using MA and green light were tested for crosslinker expansion, while reactions involving MMA and red light were tested for scaffold expansion. These reactions demonstrated the selectivity of the photoredox catalysts. The control reaction of CPD additionally serves as the assertion that the conditions of crosslinker expansion should not interfere with scaffold expansion since the presence of CPD alone does not generate polymerization. This concept of orthogonal polymerization was reinforced by the control reaction in which CPD was reacted under the conditions of crosslinker expansion, with ZnTPP under green light. There was no polymerization present, which is indicative that this RAFT reagent, when present on the scaffold, would not polymerize in the presence of ZnTPP under green light. Therefore, the polymerization conditions of the crosslinker should not affect the scaffold when ZnTPP under green light is utilized and CPD is present on the scaffold, achieving an orthogonal PGNN expansion.

2.3 Conclusion

TTC1 and TTC2 will form part of the crosslinker entities of two PGNNs. TTC1, once activated, will form part of an Ester PGNN, while TTC2 will form part of an Isocyanate PGNN. Once these crosslinkers are incorporated into nanoparticles, we plan to expand them by RAFT polymerization using ZnTPP under green light. Therefore, we evaluated the crosslinking expansion reaction of TTC1 and TTC2 outside of the nanoparticle environment to observe polymerization rate and control, and monomer conversion. For these evaluations, we conducted kinetic reactions for both TTCs under the conditions of crosslinker extension using ZnTPP under green light for MA polymerization, individually. We observed that both MA polymerizations resulted in homogenous polymers with linear MA conversion, as seen by GPC traces. Further testing with TTC1 in which a chain extension of PMA was performed demonstrated high fidelity, livingness, and narrow dispersity (Đ=1.14) of PMA with TTC1, which we expect to translate to the nanonetwork.

Several control experiments were performed to observe if the reactivities of catalysts or RAFT reagents could interfere with polymerization independently of each other. Reagents and catalysts that would be used in either scaffold or crosslinker expansions were exposed to prolonged hours to the conditions of those expansions to observe their reactivity and individual polymerization influence without each other. The results portrayed little to no polymerization of the reagents or catalysts by themselves, as observed by monomer conversion using ^{1}H NMR, apart from ZnTPP, which demonstrated a 30% monomer conversion when exposed to the reaction environment for 24 hours. These control reactions provided insight into the selectivity of the photoredox catalysts used. It was discussed the possibility of orthogonal polymerization because when the crosslinking expansion conditions were applied to the RAFT reagent present on the scaffold, no polymerization was observed.

2.4 Experimental

2.4.1 Testing Chain Extension from Crosslinkers TTC1 and TTC2 with ZnTPP

2.4.1.1 Kinetics of PMA polymerization with TTC1 and ZnTPP

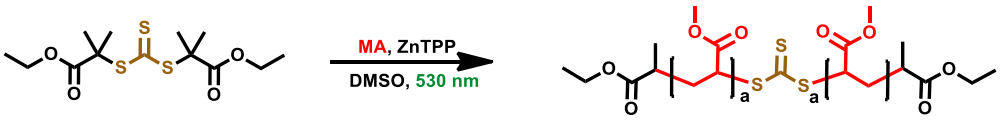

TTC1 (4.0 mg, 0.0118 mmol) was dissolved in a 2 M monomer solution of DMSO with MA (426 µL, 4.726 mmol) and ZnTPP (50 ppm to the monomer) in a 1 dram vial. The reaction vessel was sealed and sparged with nitrogen for 20 minutes. The reaction was then placed 2 cm from a 530 nm led light source and irradiated for 120 minutes. Aliquots were taken every 30 minutes for ^{1}H NMR and GPC$_{(DMF)}$ analysis. The polymer was precipitated in cold diethyl ether twice.

Minutes	MA conversion (%)	$M_{n,\,GPC}$ (g/mol)	Đ
30	39	14500	1.09
60	61	21300	1.10
90	73	25400	1.09
120	79	27400	1.09

Table S2.1: MA conversion obtained from ^{1}H NMR, molecular weight and dispersity obtained from GPC$_{(DMF)}$ traces of PMA polymerization with TTC1 and ZnTPP every 30 minutes for 2 hours

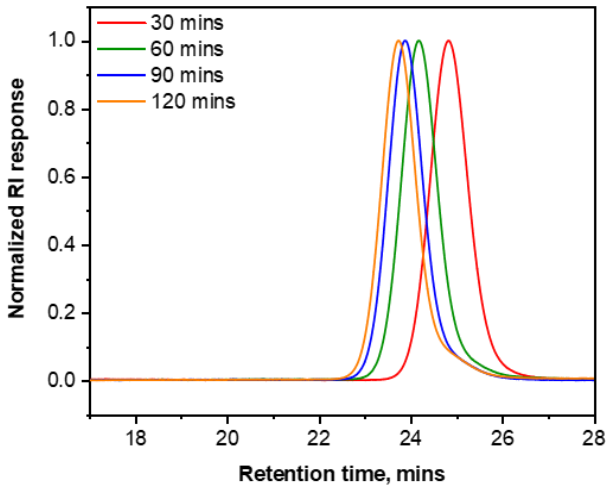

Figure S2.1: $GPC_{(DMF)}$ traces of PMA polymerization with TTC1 and ZnTPP every 30 minutes for 2 hours.

2.4.1.2 Chain extension of PMA polymerization with TTC1

PMA polymer (107.1 mg, 3.9311E-3 mmol) was dissolved in 2 M monomer solution in DMSO with MA (142 µL, 1.572 mmol) and ZnTPP (50 ppm to the monomer) in a 1 dram vial. The reaction vessel was sealed and sparged with nitrogen for 20 minutes. The reaction was then placed 2 cm from a 530 nm led light source and irradiated for 120 minutes. The polymer was precipitated in cold diethyl ether twice, and analyzed by $GPC_{(DMF)}$ ($M_{n,\ GPC}$=30600 g/mol, Đ=1.14).

2.4.1.3 Kinetics of PMA polymerization with TTC2 and ZnTPP

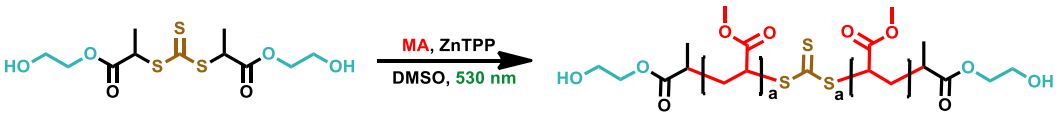

TTC2 (4.3 mg, 0.0126 mmol) was dissolved in 2 M monomer solution in DMSO with MA (452 µL, 5.0228 mmol) and ZnTPP (50 ppm to the monomer) in a 1 dram vial. The reaction vessel was sealed and sparged with nitrogen for 20 minutes. The reaction was then placed 2 cm from a

530 nm led light source and irradiated for 120 minutes. Aliquots were taken every 30 minutes for ^{1}H NMR and GPC$_{(DMF)}$ analysis. The polymer was precipitated in cold diethyl ether twice.

Minutes	MA conversion (%)	$M_{n,\,GPC}$ (g/mol)	Đ
30	39	14400	1.14
60	59	22200	1.07
90	70	25400	1.10
120	77	30400	1.10

Table S2.2: MA conversion obtained from ^{1}H NMR, molecular weight and dispersity obtained from GPC$_{(DMF)}$ traces of PMA polymerization with TTC2 and ZnTPP every 30 minutes for 2 hours

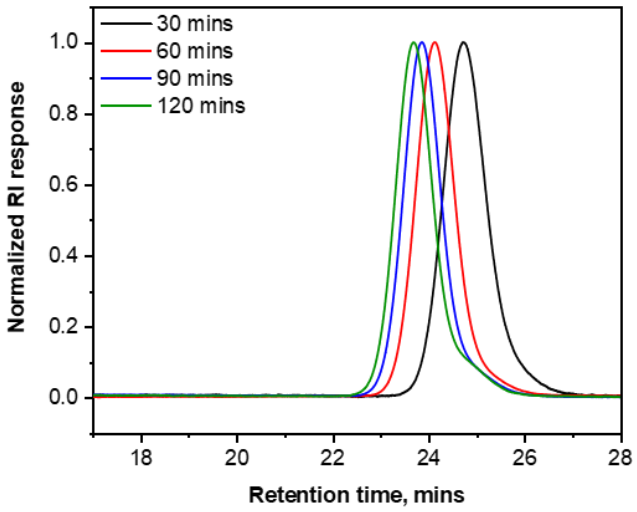

Figure S2.2: GPC$_{(DMF)}$ traces of PMA polymerization with TTC2 and ZnTPP every 30 minutes for 2 hours.

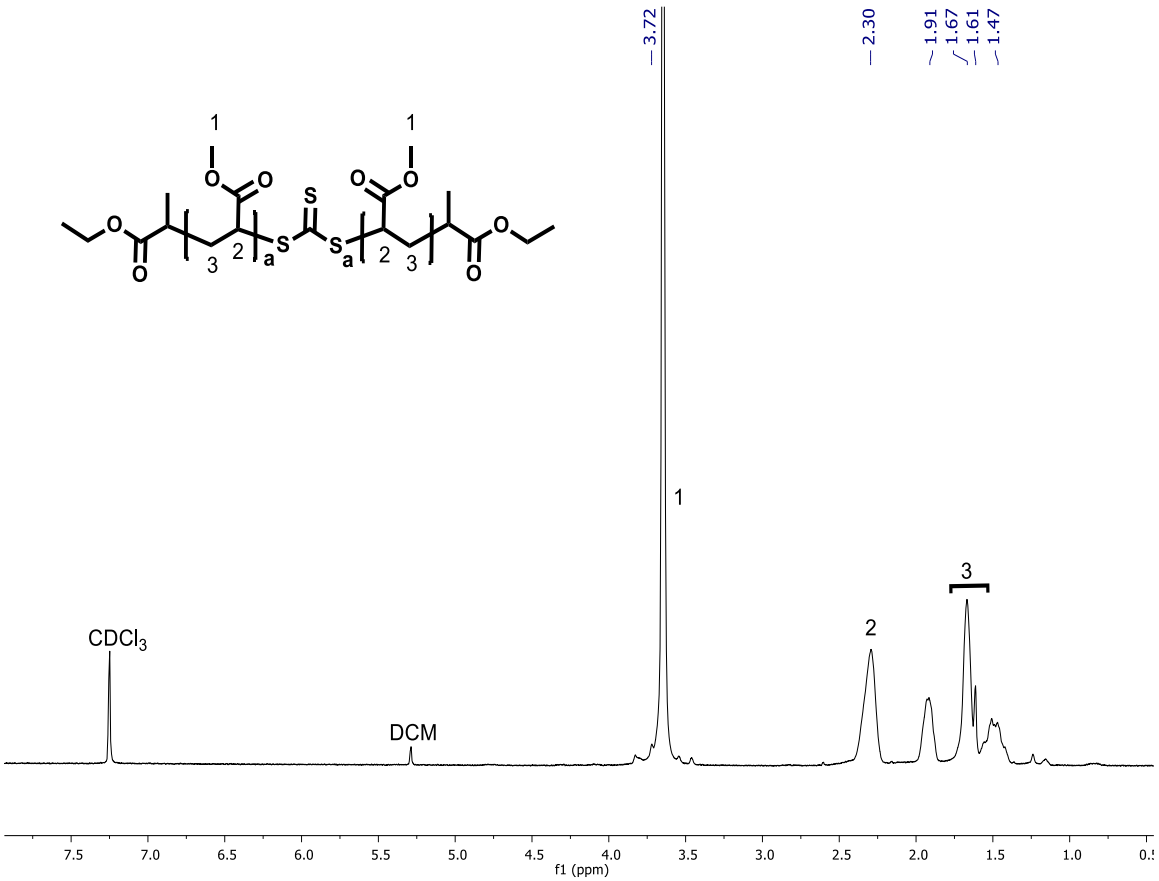

Figure S2.3: ^{1}H NMR ($CDCl_3$, 400 MHz) spectrum of PMA polymerization with TTC2 and ZnTPP.

2.4.2 Model Reactions and Control Experiments for Orthogonal Polymerization

2.4.2.1 General procedure

Following the ratio of [M]:[RAFT]:[Catalyst] to the respective monomers, RAFT reagents, and catalysts portrayed on Table S2.3, a control experiment was set up for each row of the table. The reaction vessels were sealed and sparged with nitrogen for 20 minutes. The LED light source was 2 centimeters away from the reaction vessels. For TTC1, TTC2, and CPD, 2 mg were used of the reagents while 2 mmol of PheoA and ZnTPP, on their respective reactions.

Entry	[M]:[RAFT]:[Catalyst]	M	RAFT agent	Catalyst	[Catalyst]/[M], ppm	Time, hours	α, %[c]
1[a]	400:0:0.02	MA	-	ZnTPP	50	24	30
2[a]	400:1:0	MA	TTC1	-	-	24	6
3[a]	400:1:0	MA	TTC2	-	-	24	5
4[a]	400:1:50	MA	CPD	ZnTPP	50	24	0
5[b]	400:1:0	MMA	CPD	-	-	24	0
6[b]	400:0:0.0008	MMA	-	PheoA	2	24	10

Table S2.3: Control experiments for ZnTPP regulated polymerization of MA and PheoA, regulated polymerization of MMA. *Notes*: All experiments were performed in DMSO (2 M solution of monomer). M denotes monomer. [a]Light source: green LED light (530 nm); [b]light source: red LED light (680 nm); [c]monomer conversion determined by ^{1}H NMR spectroscopy.

CHAPTER 3: ATRP Scaffolds Synthesis (PMMA-co-PHEMA)

3.1 Introduction

Transition-Metal-Catalyzed Atom Transfer Radical Polymerization (ATRP) could be used to construct block copolymers. ATRP's mechanism was derived from polymerizations that use transition metals and apply a reversible-deactivation radical polymerization (RDRP)[26]. The initial homolytic cleavage happens on the C-X bond, where X is either Br or Cl, when a metal catalyst is reduced; this initiates the polymerization[27]. The catalyst is comprised of a transition metal, copper (Cu) is usually used, that forms a halide compound along with ligands; it is utilized as an activator on the reaction[1]. Once the C-X bond is broken, the halide is transferred to another species in the system. It is possible to track the loss of chain end-groups by tracking the movement of the halogen because the loss of chain end-groups is the same as the irreversible oxidation of Cu(I) to Cu(II)[28].

The mechanism of ATRP is advantageous since it produces less termination and an equilibrium between the radical species and the dormant species. The activation and deactivation of chains decrease the amount of unnecessary active radicals and reduces the termination of chains that have not been completely extended[27]. The successive addition of monomers for one type of block, followed by another type of block seemed to be favorable for high reaction yields. The polymers formed with ATRP are noted to have low polydispersity, and well-defined block length[29]. The chain grows due to "activation-propagation-deactivation cycles" by using the metal transition catalyst[1]. The equilibrium is controlled by the choice of initiator, activator, and temperature so that the primary state is the dormant one[1].

3.2 Discussion

We decided to work with MBPA as the initiator and Me_6Tren as the ligand for the formation of an ATRP PMMA-co-PHEMA scaffold because it was established that they formed

ATRP polymers with controlled polymerization, low dispersities, and high monomer conversions[26]. DMSO was chosen as the solvent because it favors ATRP since it highly dissolves $CuBr_2$, and it favors the disproportionation reaction Cu(0)+Cu(II)=Cu(I) which increases the rate of ATRP. $CuBr_2$ is essential for ATRP due to it binds to the ligand, in this case, Me_6Tren, to donate an electron for the propagation of the chain and become Cu(I), which reacts with Cu(0) to form $CuBr_2$ again, repeating the cycle. DMSO favors these reactions.

Previously, a synthesis of PMMA-co-PICEMA, poly(methyl methacrylate)-co-poly(isocyanatoethyl methacrylate), was attempted in DMSO. However, as DMSO typically has a lot of water even when it is from an anhydrous bottle, the resulting polymers had broad dispersity or shoulders indicating coupling or crosslinking. Crosslinking is due to isocyanate reacting with water to produce amine, which can react with another isocyanate and form a urea link. Thus, the polymerization was attempted in drier solvents, such as acetonitrile and toluene; nevertheless, the reaction rate was slow because the disproportionation rate is lower and $CuBr_2$ is less soluble in those solvents. Since the reaction rate was slow, the polymers had low conversion and low yield.

Therefore, another approach was taken by functionalizing PMMA-co-PHEMA with diisocyanate. Lower percentages of HEMA polymers were synthesized since functionalization of 15% HEMA resulted in a gel. We performed three different reactions to compare the polydispersities of polymers with varying HEMA densities to use for the functionalization with diisocyanate. Our HEMA percentage targets were 15%, 10%, and 5%. GPC traces conveyed that as there was a lower HEMA density in the polymer, the dispersity lowered as well. 5% HEMA showed the lowest dispersity even with high molecular weight, which we could use to have a low density of crosslinker monomers and control the amount of reactivity on the scaffold. GPC traces also demonstrated a homogeneous polymerization with little to no termination (see Figure 3.1).

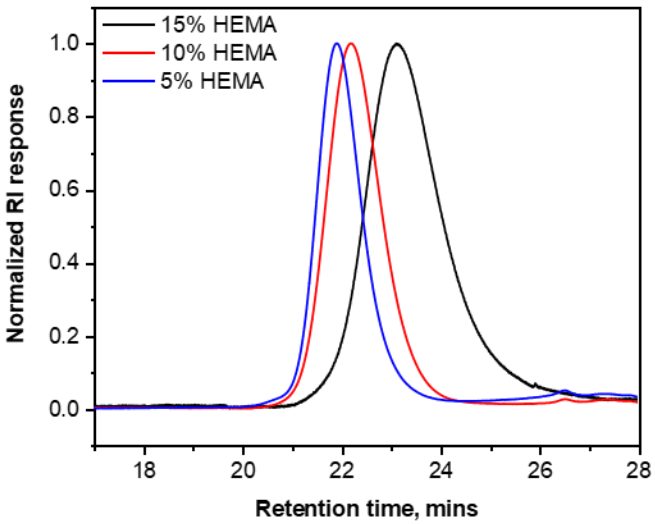

Figure 3.1: $GPC_{(THF)}$ traces of ATRP scaffold polymer with the respective HEMA percentage targets, 15% (black), 10% (red), 5% (blue).

The purpose of making this polymer was to functionalize the HEMA hydroxy group with a diisocyanate. The isocyanate would react with TTC2 to crosslink two ATRP scaffold polymers to form a nanoparticle, which could then be expanded from the scaffold through ATRP and the crosslinker through RAFT. However, once the functionalization reaction was attempted, a higher equivalency of diisocyanate was used to avoid crosslinking but purification of the polymer was difficult because unreacted diisocyanate also precipitated in ether, so not all of it could be removed. Another purification method such as dialysis would not be effective because it requires a long exposure of these polymers to a solvent that is not dry so it would most likely lead to crosslinking or isocyanates converting into amines. Thus, another approach should be taken to form the PGNN with an ATRP scaffold in order to have orthogonal expansion and better crosslinking chemistry.

3.3 Conclusion

We examined three different HEMA densities for a PMMA-co-PHEMA ATRP scaffold to study their different percentages for the functionalization with diisocyanate. ATRP has been used to generate polymers with high monomer conversion, low dispersities, and controlled

polymerization. This scaffold polymer would have been used to react the hydroxy group from the HEMA monomer with a diisocyanate to provide a way of crosslinking with TTC2. Even though the PMMA-co-PHEMA polymer demonstrated low dispersity, purification of the functionalized product was difficult.

3.4 Experimental

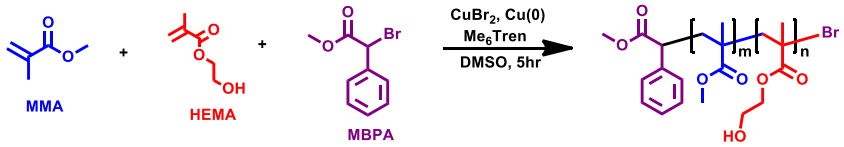

A stirrer bar wrapped with 5cm copper, Cu(0), was treated by immersion in anhydrous 37% w/v HCl, stirred for 20 minutes, sequentially washed with water and acetone, and dried. All polymerizations conducted used a MBPA/$CuBr_2$/ Me_6Tren ratio of 1/0.05/0.06. HEMA, MMA, MBPA, $CuBr_2$ from a stock solution, Me_6Tren, and DMSO (which equaled the volume of the monomers) were added into the 1 dram vial, according to the amounts portrayed on the table below. The reaction vessel was sealed and sparged with nitrogen for 15 minutes. An argon balloon was inserted. Next, the reaction was placed above a stir plate for 5 hours. The polymerization was quenched by allowing oxygen in once the vial was opened, they were precipitated in cold diethyl ether, and dried under high vacuum. The polymers were dissolved in inhibitor-free, pure THF for them to be passed through a basic aluminum oxide column to remove the copper. The solvents were removed under reduced pressure for another cold diethyl ether precipitation to which the polymer was transferred to a weighted 6 dram to be dried and characterized by $GPC_{(THF)}$ and d-DMSO ^{1}H NMR.

Target HEMA percentage →	15%		10%		5%	
Reagents ↓	Quantity	mmol	Quantity	mmol	Quantity	mmol
HEMA	201 µL	1.6568	127 µL	1.0432	59.9 µL	0.4941
MMA	1 mL	9.39	1 mL	9.39	1 mL	9.39
MBPA	26.87 µL	0.17	25 µL	0.159	23.35 µL	0.1483
$CuBr_2$	1.91 mg	0.0085	1.77 mg	0.0079	1.66 mg	0.0074
Me_6Tren	2.74 µL	0.0102	2.55 µL	0.0095	2.38 µL	0.0089

Table S3.1: Amounts and mmol of the reagents used to obtain 15%, 10%, and 5% HEMA for the ATRP scaffold

Target HEMA percentage	$M_{n,\ GPC}$ (g/mol)	Đ
15%	5000	1.24
10%	7800	1.09
5%	9100	1.07

Table S3.2: Molecular weight and dispersity obtained from $GPC_{(THF)}$ traces of ATRP scaffold according to the target HEMA percentage

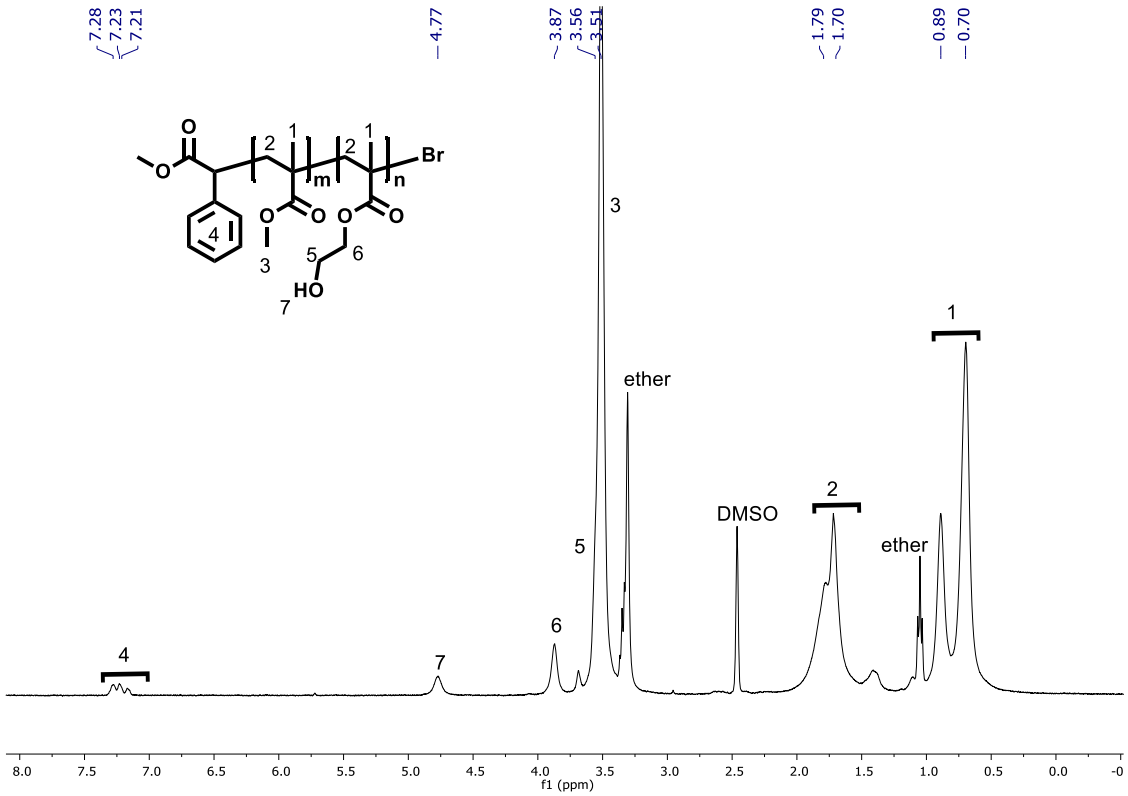

Figure S3.1: ^{1}H NMR (DMSO, 400 MHz) spectrum of the precipitated ATRP scaffold (PMMA-co-PHEMA).

GENERAL CONCLUSION

This research focused on the formation of scaffolds with varying chemistries that will interact with different symmetrical trithiocarbonate crosslinkers to form photogrowable nanonetworks. Ultimately, the end goal is to orthogonally expand these nanonetworks using photoredox catalysts from both, the scaffold and crosslinker. These expansions will be achieved by RAFT, ATRP, or ROP. These scaffolds have chemistries that contribute to crosslinking by possible esterification through acid chloride, or isocyanate-alcohol reaction, or Diels-Alder reaction. This project contributed to the construction of a RAFT scaffold which end group was removed to accommodate an ROP expansion once incorporated into a nanoparticle, a RAFT scaffold that will be expanded once incorporated into the nanoparticle by PET-RAFT polymerization with PheoA under red light, and an ATRP scaffold that would have been functionalized with diisocyanate. Pre-evaluations of TTC1 and TTC2 were conducted for polymerization behavior analysis, while control reactions were performed for the study of orthogonal polymerization.

CONFLICT OF INTEREST

The author declares no conflict of interest.

BIBLIOGRAPHY

1. Young, R. J.; Lovell, P. A. *Introduction to Polymers*, 3rd ed.; CRC Press Taylor & Francis Group, **2011**.

2. Polymer Properties Database. Block Copolymer Polymerization. http://polymerdatabase.com/ (accessed July 27, 2021).

3. Kim, J. K.; Yang, S. Y.; Lee, Y.; Kim, Y. Functional Nanomaterials Based on Block Copolymer Self-Assembly. *Progress in Polymer Science* **2010**, *35* (11), 1325–1349.

4. Feng, H.; Wang, W.; Lu, X.; Kang, N. Block Copolymers: Synthesis, Self-Assembly, and Applications. *Polymers* **2017**, *9* (10), 494.

5. Moad, G.; Rizzardo, E.; Thang, S. H. Reversible Addition Fragmentation Chain Transfer (RAFT) Polymerization. Millipore Sigma. https://www.sigmaaldrich.com/US/en/technical-documents/technical-article/materials-science-and-engineering/drug-delivery/reversible-addition (accessed July 6, 2021).

6. Parkatzidis, K.; Wang, H. S.; Truong, N. P.; Anastasaki, A. Recent Developments and Future Challenges in Controlled Radical Polymerization: A 2020 Update. *Chem* **2020**, *6* (7), 1575–1588.

7. Lampley, M. W.; Harth, E. Photocontrolled Growth of Cross-Linked Nanonetworks. *ACS Macro Letters* **2018**, *7* (6), 745-750.

8. Lampley, M. W.; Tsogtgerel, E.; Harth, E. Nanonetwork Photogrowth Expansion: Tailoring Nanoparticle Networks' Chemical Structure and Local Topology. *Polymer Chemistry* **2019**, *10* (28), 3841-3850.

9. Xu, J.; Shanmugam, S.; Fu, C.; Aguey-Zinsou, K.-F.; Boyer, C. Selective Photoactivation: From a Single Unit Monomer Insertion Reaction to Controlled Polymer Architectures. *Journal of the American Chemical Society* **2016**, *138* (9), 3094-3106.

10. Shanmugam, S.; Xu, J.; Boyer, C. Exploiting Metalloporphyrins for Selective Living Radical Polymerization Tunable over Visible Wavelengths. *Journal of the American Chemical Society* **2015**, *137* (28), 9174-9185.

11. Kwak, R. N. Y.; Matyjaszewski, K. Dibromotrithiocarbonate Iniferter for Concurrent ATRP and RAFT Polymerization. Effect of Monomer, Catalyst, and Chain Transfer Agent Structure on the Polymerization Mechanism. *Macromolecules* **2008**, *41* (13), 4585-4596.

12. Theriot, J. C.; Miyake, G. M.; Boyer, C. A. N,N-Diaryl Dihydrophenazines as Photoredox Catalysts for PET-RAFT and Sequential PET-RAFT/O-ATRP. *ACS Macro Letters* **2018**, *7* (6), 662-666.

13. Fu, C.; Xu, J.; Kokotovic, M.; Boyer, C. One-Pot Synthesis of Block Copolymers by Orthogonal Ring-Opening Polymerization and PET-RAFT Polymerization at Ambient Temperature. *ACS Macro Letters* **2016**, *5* (4), 444-449.

14. Keddie, D.J. A Guide to the Synthesis of Block Copolymers Using Reversible-Addition Fragmentation Chain Transfer (RAFT) Polymerization. *Chemical Societies Reviews* **2014**, (2), 496-505.

15. Perrier, S. 50th Anniversary Perspective: RAFT Polymerization—A User Guide. *Macromolecules* **2017**, *50* (19), 7433-7447.

16. Chen, M.; Zhong, M.; Johnson, J.A. Light-Controlled Radical Polymerization: Mechanisms, Methods, and Applications. *Chemical Reviews* **2016**, *116* (17), 10167-10211.

17. Acik, G.; Kahveci, M.U.; Yagci, Y. Synthesis of Block Copolymers by Combination of Atom Transfer Radical Polymerization and Visible Light Radical Photopolymerization Methods. *Macromolecules* **2010**, *43* (21), 9198-9201.

18. Xu, J.; Jung, K.; Atme, A.; Shanmugam, S.; Boyer, C. A Robust and Versatile Photoinduced Living Polymerization of Conjugated and Unconjugated Monomers and Its Oxygen Tolerance. *Journal of the American Chemical Society* **2014**, *136* (14), 5508–5519.

19. Phommalysack-Lovan, J.; Chu, Y.; Boyer, C.; Xu, J. PET-RAFT Polymerisation: Towards Green and Precision Polymer Manufacturing. *Chemical Communications.* **2018**, *54* (50), 6591–6606.

20. Allegrezza, M. L.; Konkolewicz, D. PET-RAFT Polymerization: Mechanistic Perspectives for Future Materials. *ACS Macro Letters* **2021**, *10* (4), 433–446.

21. Chemistry Steps. Esters Reaction with Amines – The Aminolysis Mechanism. https://www.chemistrysteps.com/esters-reaction-with-amines-the-aminolysis-mechanism/ (accessed Aug 25, 2021).

22. Qian, Y.; Dong, F.; Guo, L.; Xu, X.; Liu, H. Two-Component Waterborne Polyurethane Modified with Terpene Derivative-Based Polysiloxane for Coatings via a Thiol-Ene Click Reaction. *Industrial Crops and Products* **2021**, *171*, 113903.

23. Boyer, C.; Granville, A.; Davis, T. P.; Bulmus, V. Modification of RAFT-Polymers via Thiol-Ene Reactions: A General Route to Functional Polymers and New Architectures. *Journal of Polymer Science Part A: Polymer Chemistry* **2009**, *47* (15), 3773–3794.

24. Alsarraf, J.; Ammar, Y. A.; Robert, F.; Cloutet, E.; Cramail, H.; Landais, Y. Cyclic Guanidines as Efficient Organocatalysts for the Synthesis of Polyurethanes. *Macromolecules* **2012,** *45* (5), 2249.

25. Mavila, S.; Eivgi, O.; Berkovich, I.; Lemcoff, N. G. Intramolecular Cross-Linking Methodologies for the Synthesis of Polymer Nanoparticles. *Chemical Reviews* **2016**, *116* (3), 878–961.

26. Jones, G. R.; Whitfield, R.; Anastasaki, A.; Risangud, N.; Simula, A.; Keddie, D. J.; Haddleton, D. M. Cu(0)-RDRP of Methacrylates in DMSO: Importance of the Initiator. *Polymer Chemistry* **2018**, *9* (18), 2382–2388.

27. Messina, M. S.; Messina, K. M. M.; Bhattacharya, A.; Montgomery, H. R.; Maynard, H. D. Preparation of Biomolecule-Polymer Conjugates by Grafting-from Using ATRP, RAFT, or ROMP. *Progress in Polymer Science* **2020**, *100*, 101186.

28. Wang, Y. ATRP of Methyl Acrylate by Continuous Feeding of Activators Giving Polymers with Predictable End-Group Fidelity. *Polymers* **2019**, *11* (8), 1238.

29. Mühlebach, A.; Gaynor, S.G.; Matyjaszewski, K. Synthesis of Amphiphilic Block Copolymers by Atom Transfer Radical Polymerization (ATRP). *Macromolecules* **1998**, *31* (18), 6046-6052.